Structural Engineering and Mechanics, *Vol. 62, No. 5 (2017) 551-565*
DOI: https://doi.org/10.12989/sem.2017.62.5.551

Strain gradient theory for vibration analysis of embedded CNT-reinforced micro Mindlin cylindrical shells considering agglomeration effects

H. Tohidi[1], S.H. Hosseini-Hashemi[*1,2], A. Maghsoudpour[1] and S. Etemadi[1]

[1]*Department of Mechanical and Aerospace Engineering, Science and Research Branch, Islamic Azad University, Tehran, Iran*
[2]*School of mechanical Engineering Iran university of Science and Technology, Narmak, 16842-13114 Tehran, Iran*

(Received December 27, 2016, Revised March 23, 2017, Accepted March 30, 2017)

Abstract. Based on the strain gradient theory (SGT), vibration analysis of an embedded micro cylindrical shell reinforced with agglomerated carbon nanotubes (CNTs) is investigated. The elastic medium is simulated by the orthotropic Pasternak foundation. The structure is subjected to magnetic field in the axial direction. For obtaining the equivalent material properties of structure and considering agglomeration effects, the Mori-Tanaka model is applied. The motion equations are derived on the basis of Mindlin cylindrical shell theory, energy method and Hamilton’s principal. Differential quadrature method (DQM) is proposed to evaluate the frequency of system for different boundary conditions. The effects of different parameters such as CNTs volume percent, agglomeration of CNTs, elastic medium, magnetic field, boundary conditions, length to radius ratio and small scale parameter are shown on the frequency of the structure. The results indicate that the effect of CNTs agglomeration plays an important role in the frequency of system so that considering agglomeration leads to lower frequency. Furthermore, the frequency of structure increases with enhancing the small scale parameter.

Keywords: vibration; strain gradient theory; CNT agglomeration; micro cylindrical shell; DQM

1. Introduction

In recent years, the application of nanocomposite materials in structures has been the topic of numerous studies. Since nanocomposites have an important role in engineering structures, that's why most of the researchers were interested in nanoscience investigation in the past decades (Saito *et al*. 1998, Iijima 1991, Qian *et al*. 2004, Li and Wang 2008, Ayatollahi *et al*. 2015). CNTs have fascinating electro-thermo-mechanical properties and theyare used asbooster of the matrix phase in a composite. Such materials have extensive application in electromechanical and electrical devices such as actuators, sensors, and convertors.

It is vital for design engineers to appraise the vibration Specifications of industrial structures thoroughly and accurately. Whereas nanoshell models have extensive applications in nanoelectromechanical systems, actuators, biomedical sensors, and the transfer of electricity in electronic nanodevices. So a large number of investigations are carried out to cylindrical shells such as free vibration (Paliwal *et al*. 1996) and forced vibration (Rogacheva 1988). The majority of the studies are based on classical continuous theories like classical theory, first order shear deformation theory (FSDT), high order shear deformation theory (TSDT) and high order shear deformation theory (HSDT), which the following refers to them. Shen and Xiang (2012) accomplished the nonlinear vibration of nanotube reinforced composite cylindrical shells in thermal environments. The motion equations are based on a higher-order shear deformation theory. The results show that the natural frequencies are reduced but the nonlinear to linear frequency ratios are increased by increasing the temperature. The same authors (Shen and Xiang 2014) analyzed the nonlinear vibration of nanotube reinforced composite cylindrical panels resting on elastic foundations in thermal environments. The equations of motion are solved by a two-step perturbation technique to determine the nonlinear frequencies of the CNTRC panels. Numerical results demonstrate that the natural frequencies of the CNTRC panels are reduced but the nonlinear to linear frequency ratios of the CNTRC panels are increased as the temperature rises. In contrast, natural frequencies are increased but the nonlinear to linear frequency ratios are decreased by increasing the foundation stiffness. Changcheng and Yinghui (2013) examined the Nonlinear dynamic analysis of Sigmoid functionally graded circular cylindrical shells on elastic foundations using the third order shear deformation theory in thermal environments. The Galerkin method and fourth-order Runge-Kutta method are used to calculate natural frequencies, nonlinear frequency-amplitude relation and dynamic response of the shells. Yas *et al*. (2013) presented the three-dimensional free vibration analysis of functionally graded nanocomposite cylindrical panels reinforced by carbon nanotube. The motion equations are solved by generalized differential quadrature (GDQ) method. Alibeigloo (2014) reported the Free vibration analysis of functionally graded carbon nanotube reinforced composite cylindrical panel embedded in piezoelectric layers by using theory of elasticity. The boundary conditions are assumed to be

∗Corresponding author
E-mail: shh@iust.ac.ir

http://www.techno-press.com/journals/sem&subpage=7 ISSN: 1225-4568 (Print), 1598-6217 (Online)

simply supported. By using Fourierseries expansion along the longitudinal and latitudinal directions and state space technique across the thickness direction, state space differential equations are solved analytically. Zhang et al. (2015a) studied the Vibration analysis of functionally graded carbon nanotube reinforced composite thick plates with elastically restrained edges. Mirzae and Kiani (2016) proposed the Free Vibration of Functionally graded carbon nanotube reinforced composite cylindrical panels. Numerical results reveal that, frequencies of the panel are dependent to both, volume fraction of carbon nanotubes and their distribution pattern across the thickness. Civalek (2016) studied the free vibration of carbon nanotubes reinforced (CNTR) and functionally graded shells and plates based on FSDT via discrete singular convolution method. To obtain the eigenvalue problem of the system, the method of discrete singular convolution is employed. Five types of distributions of CNTR material are also considered. Song *et al*. (2016) analyzed the Vibration analysis of CNT-reinforced functionally graded composite cylindrical shells in thermal environments. Vibration responses of the cylindrical shell are computed by using the FSDT and TSDT. The results show that the strengthening of the stiffness near the surfaces of CNT reinforced functionally graded cylindrical shell is more effective in reducing the vibration amplitude of the structure. Gharib *et al*. (2016) proposed the vibration analysis of the embedded piezoelectric polymeric nanocomposite panels in the elastic substrate. The micro-panel is considered as the thin wall shell and Donnell's non-linear theory is used for the strain-displacement relations. Stiffness of the panel is reduced by increasing length to radius ratio and reducing density and lower frequencies are obtained.

Experimental studies have shown that the material elastic constants have intense dependency on structural dimensions at the micro/nano-scale. As the structure dimensions are scaled down, with regarding to size reduction which is known size effect, the stiffness and resistance of material will increase. Whereas the study of nanoshells is concerned with nano dimensions, the classical theory can't anticipate structural behavior precisely. Because the classical theory of continuum mechanic cannot consider the small-scale size effects hence with considering thesize effect, higher order continuum theories are applied. The mentioned theories consist the nonlocal elasticity theory, the modified couple stress theory (MCST), the modified SGT and the surface elasticity theory. Different researches have been accomplished in the field of non classical small-scale such as shell, beam and plate. For example, based on the strain gradient and Eringen's piezoelasticity theories, wave propagation of an embedded double-walled boron nitride nanotube (DWBNNT) conveying fluid was investigated by Ghorbanpour Arani *et al*. (2012) using Euler-Bernoulli beam model. Li *et al*. (2013) concerned with transverse vibrations of axially traveling nanobeams including strain gradient and thermal effects. The strain gradient elasticity theory and the temperature field were taken into consideration. The buckling problem of linearly tapered micro-columns was investigated by Akgoz and Civalek (2013) on the basis of modified strain gradient elasticity theory. Bernoulli-Euler beam theory is used to model the non-uniform micro column. Tadi Beni *et al*. (2014) investigated the free vibration analysis of size-dependent shear deformation functionally graded cylindrical shell on the basis of MCST. The free vibration of simply supported functionally graded cylindrical nanoshell were obtained, and the effects of parameters such as dimensionless length scale parameter, distribution of FG properties, thickness, and length on the natural frequency were identified. Zeighampour *et al*. (2014) studied the cylindrical thin-shell model based on modified SGT. The findings indicate that the rigidity of the nanoshell in the modified SGT is greater than that in couple stress model and the classical theory, which leads to the increase in natural frequencies. Zhang *et al*. (2015b) presented the free vibration analysis of four-unknown shear deformable functionally graded cylindrical microshells based on the strain gradient elasticity theory. Numerical results indicate that both the frequency and higher-order mode shapes exhibit significant size-dependence when the thickness of the microshell approaches to the material length scale parameter. Based on the strain gradient elasticity theory and a refined shear deformation theory, an efficient size-dependent plate model was developed by Zhang *et al*. (2015c) to analysis the bending, buckling and free vibration problems of functionally graded microplates resting on elastic foundation. Gholami *et al*. (2016) analyzed the Vibration and buckling of first-order shear deformable circular cylindrical micro-/nano-shells based on Mindlin's strain gradient elasticity theory. The motion equations are analyzed by employing a Navier-type solution. It is shown that the effect of small scale is more prominent for lower values of dimensionless length scale parameter. Li and Hu (2016) investigated the wave propagation in fluid-conveying viscoelastic carbon nanotubes based on nonlocal SGT. It is shown that the effects of nonlocal parameters and small scale material parameters on the dispersion relation between the phase velocity and the wave number are significant at high wave numbers, however, may be ignored at low wave numbers. New torsional models of carbon nanotube in which axial velocity and the velocity gradient effect were separately considered on the basis of newly proposed nonlocal strain gradient theory were presented bu Guo *et al*. (2016). Ansari *et al*. (2016) reported the Size dependent thermomechanical vibration and instability of conveying fluid functionally graded nanoshells based on Mindlin's SGT. The results showed that at small values of dimensionless length scale parameters, there are significant differences between the natural frequencies, critical flow velocities and instability region obtained from SGT and CT. Razavi *et al*. (2016) performed the Free vibration analysis of functionally graded piezoelectric cylindrical nanoshell based on consistent couple stress theory. It is demonstrated that the length-to-radius ratio, radius-to thickness ratio, and dimensionless length scale parameter play a significant role in the vibration behavior of the FGPM cylindrical nanoshell based on the size-dependent piezoelectric theory. The size-dependent elasticity of a series of nickel cantilever microbeams was investigated experimentally by Lei (2016) based on SGT and DQM.

However, to date, no report has been found in the literature on the vibration behavior of a micro cylindrical shell reinforced with agglomerated CNTs. This paper aims to study of vibration analysis in micro cylindrical shells reinforced with CNTs considering agglomeration effects based on Mori-Tanaka model. The structure is surrounded by the orthotropic Pasternak foundation and is subjected to magnetic field. Size effects are considered by the SGT. Using Hamilton's principle and Mindlin cylindrical shell theory, the motion equations are derived and solved by DQM. The effects of CNTs volume percent, agglomeration of CNTs, elastic medium, magnetic field, boundary conditions, length to radius ratio and small scale parameter are shown on the frequency of the nanocomposite micro cylindrical shell.

2. Formulation

Fig. 1 illustrates the embedded micro cylindrical shell reinforced with agglomerated CNTs in which geometrical parameters of radius, R, length, L, and thickness h are also indicated. The structure is subjected to axial magnetic field and the surrounding elastic medium is modeled by spring and shear constants.

2.1 Strain gradient theory

Based on the SGT, the potential energy can be considered as function of the symmetric strain tensor, the dilatation gradient vector, the deviatoric stretch gradient tensor and the symmetric rotation gradient tensor. In the mentioned tensors and vectors, three independent material length scale parameters are existed. However, the potential energy U can be expressed as follows (Li and Hu 2016)

$$U=\frac{1}{2}\int_V\left(\sigma_{ij}\varepsilon_{ij}+P_i\gamma_i+\tau_{ijk}{}^{(1)}\eta_{ijk}{}^{(1)}+m_{ij}{}^{s}\chi_{ij}{}^{s}\right)dV\,, \tag{1}$$

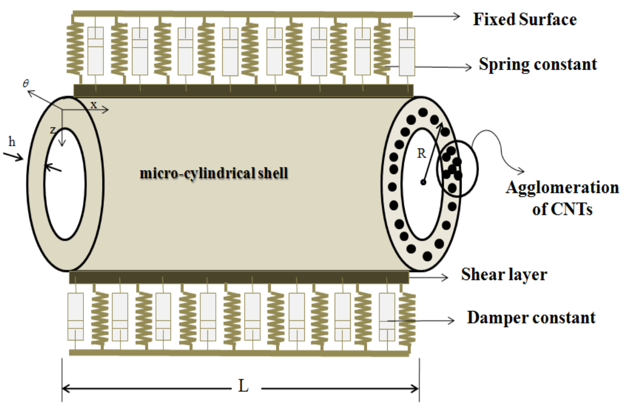

Fig. 1 A schematic figure for embedded micro cylindrical shell reinforced with agglomerated CNTs subjected to axial magnetic field

where $\varepsilon_{ij}, \gamma_i,\ \eta_{ijk}^{(1)}$ and χ_{ij} denote the strain tensor, the dilatation gradient vector, the deviatoric stretch gradient and the symmetric rotation gradient tensors, respectively, which are defined by (Li and Hu 2016, Razavi *et al*. 2016)

$$\varepsilon_{ij}=\frac{1}{2}\left(u_{i,j}+u_{j,i}\right), \tag{2}$$

$$\gamma_i=\varepsilon_{mm,i}\,, \tag{3}$$

$$\begin{aligned}\eta_{ijk}&=\frac{1}{3}\left(\varepsilon_{jk,i}+\varepsilon_{ki,j}+\varepsilon_{ij,k}\right)-\frac{1}{15}\delta_{ij}\left(\varepsilon_{mm,k}+2\varepsilon_{mk,m}\right)\\&-\frac{1}{15}\left[\delta_{jk}\left(\varepsilon_{mm,i}+2\varepsilon_{mi,m}\right)+\delta_{ki}\left(\varepsilon_{mm,j}+2\varepsilon_{mj,m}\right)\right],\end{aligned} \tag{4}$$

$$\chi_{ij}{}^{s}=\frac{1}{2}\left(\theta_{i,j}+\theta_{j,i}\right), \tag{5}$$

where u_i and δ_{ij} are the displacement vector and the knocker delta, respectively. In addition, the rotation vector (θ_i) can be defined as

$$\theta_i=\left(\frac{1}{2}curl\left(u\right)\right)_i. \tag{6}$$

The classical stress tensor, σ_{ij} , the higher-order stresses, p_i, $\tau_{ijk}^{(1)}$ and m_{ij} can be given by

$$\sigma_{ij}=\lambda tr\,\varepsilon\delta_{ij}+2\mu\varepsilon_{ij}\,, \tag{7}$$

$$p_i=2\mu l_0^2\gamma_i\,, \tag{8}$$

$$\tau^{1}{}_{ijk}=2\mu l_1^2\eta_{ijk}^1\,, \tag{9}$$

$$m_{ij}^s=2\mu l_2^2\chi_{ij}^s\,, \tag{10}$$

where λ and μ are the bulk and shear modulus, respectively; (l_0,l_1,l_2) are independent material length scale parameters.

2.2 Mindlin cylindrical shell

The displacement fields in the Mindlin theory can be described as (Reddy 2002)

$$U\left(x,\theta,z,t\right)=u_0\left(x,\theta,t\right)+z\,\phi_x\left(x,\theta,t\right), \tag{11}$$

$$V\left(x,\theta,z,t\right)=v_0\left(x,\theta,t\right)+z\,\phi_\theta\left(x,\theta,t\right), \tag{12}$$

$$W\left(x,\theta,z,t\right)=w_0\left(x,\theta,t\right), \tag{13}$$

where (u_0, v_0, w_0) are the axial, circumferential and transverse displacements on the mid-plane (i.e., $z = 0$) of the shell; ϕ_x and ϕ_θ are the rotations of the normal to the mid-plane about x- and θ - directions, respectively. Substituting Eq. (12) into Eq. (2), the non-zero strains are

$$\varepsilon_{xx} = \frac{\partial u_0}{\partial x} + z\frac{\partial \phi_x}{\partial x}, \tag{14a}$$

$$\varepsilon_{\theta\theta} = \frac{1}{r}\left(\frac{\partial v_0}{\partial \theta} + z\frac{\partial \phi_\theta}{\partial \theta} + w_0\right), \tag{14b}$$

$$\varepsilon_{x\theta} = \frac{1}{2}\left(\frac{\partial v_0}{\partial x} + z\frac{\partial \phi_\theta}{\partial x} + \frac{1}{r}\frac{\partial u_0}{\partial \theta} + \frac{z}{r}\frac{\partial \phi_x}{\partial \theta}\right), \tag{14c}$$

$$\varepsilon_{xz} = \frac{1}{2}\left(\frac{\partial w_0}{\partial x} + \phi_x\right), \tag{14d}$$

$$\varepsilon_{\theta z} = \frac{1}{2}\left(\frac{1}{r}\frac{\partial w_0}{\partial \theta} + \phi_\theta - \frac{v_0}{r}\right). \tag{14e}$$

Substituting Eqs. (14) into Eqs. (2)-(5), the non-zero components of the dilatation gradient vector, the deviatoric stretch gradient and the symmetric rotation gradient tensors can be expressed as

$$\gamma_x = \frac{\partial^2 u_0}{\partial x^2} + z\frac{\partial^2 \phi_x}{\partial x^2} + \frac{1}{r}\frac{\partial^2 v_0}{\partial x\partial\theta} + \frac{z}{r}\frac{\partial^2 \phi_\theta}{\partial x\partial\theta} + \frac{1}{r}\frac{\partial w_0}{\partial x}, \tag{15a}$$

$$\gamma_\theta = \frac{\partial^2 u_0}{\partial x\partial\theta} + z\frac{\partial^2 \phi_x}{\partial x\partial\theta} + \frac{1}{r}\frac{\partial^2 v_0}{\partial\theta^2} + \frac{z}{r}\frac{\partial^2 \phi_\theta}{\partial\theta^2} + \frac{1}{r}\frac{\partial w_0}{\partial\theta}, \tag{15b}$$

$$\gamma_z = \frac{\partial \phi_x}{\partial x} + \frac{1}{r}\frac{\partial \phi_\theta}{\partial \theta}. \tag{15c}$$

$$\begin{aligned}\eta_{xxx} &= \frac{2}{5}\frac{\partial^2 u_0}{\partial x^2} + \frac{2}{5}z\frac{\partial^2 \phi_x}{\partial x^2} - \frac{1}{5r}\frac{\partial^2 v_0}{\partial x\partial\theta} - \frac{z}{5r}\frac{\partial^2 \phi_\theta}{\partial x\partial\theta} \\ &-\frac{1}{5r}\frac{\partial w_0}{\partial x} - \frac{1}{5}\frac{\partial^2 v_0}{\partial x\partial\theta} - \frac{z}{5}\frac{\partial^2 \phi_\theta}{\partial x\partial\theta} - \frac{1}{5r}\frac{\partial^2 u_0}{\partial\theta^2} - \frac{z}{5r}\frac{\partial^2 \phi_x}{\partial\theta^2},\end{aligned} \tag{16a}$$

$$\begin{aligned}\eta_{\theta\theta\theta} &= \frac{2}{5r}\frac{\partial^2 v_0}{\partial\theta^2} + \frac{2z}{5r}\frac{\partial^2 \phi_\theta}{\partial\theta^2} + \frac{2}{5r}\frac{\partial w_0}{\partial\theta} - \frac{1}{5}\frac{\partial^2 u_0}{\partial x\partial\theta} \\ &-\frac{z}{5}\frac{\partial^2 \phi_x}{\partial x\partial\theta} - \frac{1}{5}\frac{\partial^2 v_0}{\partial x\partial\theta} - \frac{z}{5}\frac{\partial^2 \phi_\theta}{\partial x\partial\theta} - \frac{1}{5r}\frac{\partial^2 u_0}{\partial\theta^2} - \frac{z}{5r}\frac{\partial^2 \phi_x}{\partial\theta^2},\end{aligned} \tag{16b}$$

$$\eta_{zzz} = -\frac{1}{5}\frac{\partial^2 w_0}{\partial x^2} - \frac{1}{5}\frac{\partial \phi_x}{\partial x} - \frac{1}{5r}\frac{\partial^2 w_0}{\partial\theta^2} - \frac{1}{5}\frac{\partial \phi_\theta}{\partial\theta}, \tag{16c}$$

$$\begin{aligned}\eta_{xx\theta} = \eta_{x\theta x} = \eta_{\theta xx} &= \frac{4}{15}\frac{\partial^2 v_0}{\partial x^2} + \frac{4z}{15}\frac{\partial^2 \phi_\theta}{\partial x^2} \\ &+\frac{4}{15r}\frac{\partial^2 u_0}{\partial x\partial\theta} + \frac{4z}{15r}\frac{\partial^2 \phi_x}{\partial x\partial\theta} + \frac{4}{15}\frac{\partial^2 u_0}{\partial x\partial\theta} + \frac{4z}{15}\frac{\partial^2 \phi_x}{\partial x\partial\theta} \\ &-\frac{1}{5r}\frac{\partial^2 v_0}{\partial\theta^2} - \frac{z}{5r}\frac{\partial^2 \phi_\theta}{\partial\theta^2} - \frac{1}{5r}\frac{\partial w_0}{\partial\theta},\end{aligned} \tag{16d}$$

$$\begin{aligned}\eta_{xxz} = \eta_{xzx} = \eta_{zxx} &= \frac{4}{15}\frac{\partial w_0}{\partial x} + \frac{4}{15}\frac{\partial \phi_x}{\partial x} \\ &-\frac{1}{15r}\frac{\partial^2 w_0}{\partial\theta^2} - \frac{1}{15}\frac{\partial \phi_\theta}{\partial\theta},\end{aligned} \tag{16e}$$

$$\begin{aligned}\eta_{\theta\theta x} = \eta_{\theta x\theta} = \eta_{x\theta\theta} &= \frac{4}{15}\frac{\partial^2 v_0}{\partial x\partial\theta} + \frac{4}{15}z\frac{\partial^2 \phi_\theta}{\partial x\partial\theta} \\ &+\frac{4}{15r}\frac{\partial^2 u_0}{\partial\theta^2} + \frac{4z}{15r}\frac{\partial^2 \phi_x}{\partial\theta^2} + \frac{4}{15r}\frac{\partial^2 v_0}{\partial x\partial\theta} + \frac{4z}{15r}\frac{\partial^2 \phi_\theta}{\partial x\partial\theta} \\ &+\frac{4}{15r^2}\frac{\partial w_\theta}{\partial x} - \frac{2}{15}\frac{\partial^2 u_0}{\partial x^2} - \frac{2z}{15}\frac{\partial^2 \phi_x}{\partial x^2},\end{aligned} \tag{16f}$$

$$\begin{aligned}\eta_{\theta\theta z} = \eta_{z\theta z} = \eta_{z\theta\theta} &= \frac{4}{15r}\frac{\partial^2 w_0}{\partial\theta^2} + \frac{4}{15}\frac{\partial \phi_\theta}{\partial\theta} \\ &-\frac{1}{15}\frac{\partial^2 w_0}{\partial x^2} - \frac{1}{15}\frac{\partial \phi_x}{\partial x},\end{aligned} \tag{16g}$$

$$\begin{aligned}\eta_{zzx} = \eta_{zxz} = \eta_{xzz} &= -\frac{1}{5}\frac{\partial^2 u_0}{\partial x^2} - \frac{z}{5}\frac{\partial^2 \phi_x}{\partial x^2} \\ &-\frac{1}{15r}\frac{\partial^2 v_0}{\partial x\partial\theta} - \frac{z}{15r}\frac{\partial^2 \phi_\theta}{\partial x\partial\theta} - \frac{1}{15r}\frac{\partial w_0}{\partial x} \\ &-\frac{1}{15}\frac{\partial^2 v_0}{\partial x\partial\theta} - \frac{z}{15}\frac{\partial^2 \phi_\theta}{\partial x\partial\theta} - \frac{1}{15r}\frac{\partial^2 u_0}{\partial\theta^2} - \frac{z}{15r}\frac{\partial^2 \phi_x}{\partial\theta^2},\end{aligned} \tag{16h}$$

$$\begin{aligned}\eta_{zz\theta} = \eta_{z\theta z} = \eta_{\theta zz} &= -\frac{1}{5r}\frac{\partial^2 v_0}{\partial\theta^2} - \frac{z}{5r}\frac{\partial^2 \phi_\theta}{\partial\theta^2} \\ &-\frac{1}{5r}\frac{\partial w_0}{\partial\theta} - \frac{1}{15}\frac{\partial^2 u_0}{\partial x\partial\theta} - \frac{z}{15}\frac{\partial^2 \phi_x}{\partial x\partial\theta} - \frac{1}{15}\frac{\partial^2 v_0}{\partial x^2} \\ &-\frac{z}{15}\frac{\partial^2 \phi_\theta}{\partial x^2} - \frac{1}{15r}\frac{\partial^2 u_0}{\partial x\partial\theta} - \frac{z}{15r}\frac{\partial^2 \phi_x}{\partial x\partial\theta},\end{aligned} \tag{16i}$$

$$\begin{aligned}\eta_{x\theta z} = \eta_{\theta zx} = \eta_{zx\theta} &= \frac{1}{6r}\frac{\partial^2 w_0}{\partial x\partial\theta} + \frac{1}{6}\frac{\partial \phi_\theta}{\partial x} \\ &+\frac{1}{6}\frac{\partial^2 w_0}{\partial x\partial\theta} + \frac{1}{6}\frac{\partial \phi_x}{\partial\theta},\end{aligned} \tag{16j}$$

$$\chi_{xx} = \frac{1}{2}\left[\frac{1}{r}\frac{\partial v_0}{\partial x} + \frac{z}{r}\frac{\partial \phi_\theta}{\partial x} + \frac{\partial \phi_\theta}{\partial x} - \frac{1}{r}\frac{\partial^2 w_0}{\partial x\partial\theta}\right], \tag{17a}$$

$$\chi_{\theta\theta} = \frac{1}{2r}\begin{bmatrix} \dfrac{\partial^2 w_0}{\partial x\,\partial\theta} - \dfrac{\partial\phi_x}{\partial\theta} - \dfrac{\partial v_0}{\partial x} - z\,\dfrac{\partial\phi_\theta}{\partial x} \\ +\dfrac{1}{r}\dfrac{\partial u_0}{\partial\theta} + \dfrac{z}{r}\dfrac{\partial\phi_x}{\partial\theta} \end{bmatrix}, \tag{17b}$$

$$\chi_{x\theta} = \frac{1}{4}\begin{bmatrix} \dfrac{\partial^2 w_0}{\partial x^2} - \dfrac{\partial\phi_x}{\partial x} + \dfrac{1}{r^2}\dfrac{\partial v_0}{\partial\theta} - \dfrac{1}{r^2}\dfrac{\partial^2 w_0}{\partial\theta^2} \\ +\dfrac{z}{r^2}\dfrac{\partial\phi_\theta}{\partial\theta} + \dfrac{1}{r}\dfrac{\partial\phi_\theta}{\partial\theta} \end{bmatrix}, \tag{17c}$$

$$\chi_{xz} = \frac{1}{4}\begin{bmatrix} -\dfrac{\partial^2 v_0}{\partial x^2} - z\,\dfrac{\partial^2\phi_\theta}{\partial x^2} + \dfrac{1}{r}\dfrac{\partial^2 u_0}{\partial x\,\partial\theta} \\ +\dfrac{z}{r}\dfrac{\partial^2\phi_x}{\partial x\,\partial\theta} + \dfrac{1}{r}\phi_\theta \end{bmatrix}, \tag{17d}$$

$$\chi_{\theta z} = \frac{1}{4}\begin{bmatrix} -\dfrac{1}{r}\dfrac{\partial w_0}{\partial x} + \dfrac{1}{r}\phi_x - \dfrac{1}{r}\dfrac{\partial^2 v_0}{\partial x\,\partial\theta} \\ -\dfrac{z}{r}\dfrac{\partial^2\phi_\theta}{\partial x\,\partial\theta} + \dfrac{1}{r^2}\dfrac{\partial^2 u_0}{\partial\theta^2} + \dfrac{z}{r^2}\dfrac{\partial^2\phi_x}{\partial\theta^2} \end{bmatrix}, \tag{17e}$$

$$\chi_{zz} = \frac{1}{2}\left[-\frac{\partial\phi_\theta}{\partial x} + \frac{1}{r}\frac{\partial\phi_x}{\partial\theta}\right]. \tag{17f}$$

Substituting the non-zero strain gradients detailed in Eqs. (14)-(17) into Eqs. (7)-(10), the non-zero stresses can be written as

$$\begin{aligned}\sigma_{xx} &= \frac{E}{1-\nu^2}\left(\varepsilon_{xx} + \nu\varepsilon_{\theta\theta}\right) \\ &= \frac{E}{1-\nu^2}\left[\frac{\partial u_0}{\partial x} + z\,\frac{\partial\phi_x}{\partial x} + \frac{\nu}{r}\left(\frac{\partial v_0}{\partial\theta} + z\,\frac{\partial\phi_\theta}{\partial\theta} + w_0\right)\right],\end{aligned} \tag{18a}$$

$$\begin{aligned}&\sigma_{\theta\theta} = \frac{E}{1-\nu^2}\left(\varepsilon_{\theta\theta} + \nu\varepsilon_{xx}\right) = \\ &\frac{E}{1-\nu^2}\left[\frac{1}{r}\left(\frac{\partial v_0}{\partial\theta} + z\,\frac{\partial\phi_\theta}{\partial\theta} + w_0\right) + \nu\left(\frac{\partial u_0}{\partial x} + z\,\frac{\partial\phi_x}{\partial x}\right)\right],\end{aligned} \tag{18b}$$

$$\tau_{x\theta} = 2\mu\varepsilon_{x\theta} = \mu\left[\frac{\partial v_0}{\partial x} + z\,\frac{\partial\phi_\theta}{\partial x} + \frac{1}{r}\frac{\partial u_0}{\partial\theta} + \frac{z}{r}\frac{\partial\phi_x}{\partial\theta}\right], \tag{18c}$$

$$\tau_{xz} = 2\mu\varepsilon_{xz} = \mu\left[\frac{\partial w_0}{\partial x} + \phi_x\right], \tag{18d}$$

$$\tau_{\theta z} = 2\mu\varepsilon_{\theta z} = \mu\left[\frac{1}{r}\frac{\partial w_0}{\partial\theta} + \phi_\theta - \frac{v_0}{r}\right], \tag{18e}$$

$$\begin{aligned}&p_x = 2\mu l_0^2\gamma_x = \\ &2\mu l_0^2\left(\frac{\partial^2 u_0}{\partial x^2} + z\,\frac{\partial^2\phi_x}{\partial x^2} + \frac{1}{r}\frac{\partial^2 v_0}{\partial x\,\partial\theta} + \frac{z}{r}\frac{\partial^2\phi_\theta}{\partial\theta\partial x} + \frac{1}{r}\frac{\partial w_0}{\partial x}\right),\end{aligned} \tag{19a}$$

$$\begin{aligned}&p_\theta = 2\mu l_0^2\gamma_\theta = \\ &2\mu l_0^2\left(\frac{1}{r}\frac{\partial^2 u_0}{\partial x\,\partial\theta} + \frac{z}{r}\frac{\partial^2\phi_x}{\partial x\,\partial\theta} + \frac{1}{r^2}\frac{\partial^2 v_0}{\partial\theta^2} + \frac{z}{r^2}\frac{\partial^2\phi_\theta}{\partial\theta^2} + \frac{1}{r^2}\frac{\partial w_0}{\partial\theta}\right),\end{aligned} \tag{19b}$$

$$p_z = 2\mu l_0^2\gamma_z = 2\mu l_0^2\left(\frac{\partial\phi_x}{\partial x} + \frac{1}{r}\frac{\partial\phi_\theta}{\partial\theta}\right), \tag{19c}$$

$$\begin{aligned}\tau_{xxx} &= 2\mu l_1^2\eta_{xxx} = 2\mu l_1^2\left(\frac{2}{5}\frac{\partial^2 u_0}{\partial x^2} + \frac{2}{5}z\,\frac{\partial^2\phi_x}{\partial x^2}\right. \\ &-\frac{1}{5r}\frac{\partial^2 v_0}{\partial x\,\partial\theta} - \frac{z}{5r}\frac{\partial^2\phi_\theta}{\partial x\,\partial\theta} - \frac{1}{5r}\frac{\partial w_0}{\partial x} - \frac{1}{5r}\frac{\partial^2 v_0}{\partial x\,\partial\theta} \\ &\left.-\frac{z}{5r}\frac{\partial^2\phi_\theta}{\partial x\,\partial\theta} - \frac{1}{5r^2}\frac{\partial^2 u_0}{\partial\theta^2} - \frac{z}{5r^2}\frac{\partial^2\phi_x}{\partial\theta^2}\right),\end{aligned} \tag{20a}$$

$$\begin{aligned}\tau_{\theta\theta\theta} &= 2\mu l_1^2\eta_{\theta\theta\theta} = 2\mu l_1^2\left(\frac{2}{5r^2}\frac{\partial^2 v_0}{\partial\theta^2} + \frac{2z}{5r^2}\frac{\partial^2\phi_\theta}{\partial\theta^2}\right. \\ &+\frac{2}{5r^2}\frac{\partial w_0}{\partial\theta} - \frac{1}{5r}\frac{\partial^2 u_0}{\partial x\,\partial\theta} - \frac{z}{5r}\frac{\partial^2\phi_x}{\partial x\,\partial\theta} - \frac{1}{5}\frac{\partial^2 v_0}{\partial x^2} \\ &\left.-\frac{z}{5}\frac{\partial^2\phi_\theta}{\partial x^2} - \frac{1}{5r}\frac{\partial^2 u_0}{\partial x\,\partial\theta} - \frac{z}{5r}\frac{\partial^2\phi_x}{\partial x\,\partial\theta}\right),\end{aligned} \tag{20b}$$

$$\begin{aligned}&\tau_{zzz} = 2\mu l_1^2\eta_{zzz} = 2\mu l_1^2 = \\ &\left(-\frac{1}{5}\frac{\partial^2 w_0}{\partial x^2} - \frac{2}{5}\frac{\partial\phi_x}{\partial x} - \frac{1}{5r^2}\frac{\partial^2 w_0}{\partial\theta^2} - \frac{2}{5r}\frac{\partial\phi_\theta}{\partial\theta} + \frac{1}{5r^2}\frac{\partial v_0}{\partial\theta}\right),\end{aligned} \tag{20c}$$

$$\begin{aligned}&\tau_{x\theta z} = 2\mu l_1^2\eta_{x\theta z} = \\ &2\mu l_1^2\left(\frac{1}{6r}\frac{\partial^2 w_0}{\partial x\,\partial\theta} + \frac{1}{3}\frac{\partial\phi_\theta}{\partial x} + \frac{1}{6r}\frac{\partial^2 w_0}{\partial\theta\partial x} + \frac{1}{3r}\frac{\partial\phi_x}{\partial\theta} - \frac{1}{6r}\frac{\partial v_0}{\partial x}\right),\end{aligned} \tag{20d}$$

$$\begin{aligned}\tau_{xx\theta} &= 2\mu l_1^2\eta_{xx\theta} = 2\mu l_1^2\left(\frac{4}{15}\frac{\partial^2 v_0}{\partial x^2} + \frac{4z}{15}\frac{\partial^2\phi_\theta}{\partial x^2}\right. \\ &+\frac{4}{15r}\frac{\partial^2 u_0}{\partial x\,\partial\theta} + \frac{4z}{15r}\frac{\partial^2\phi_x}{\partial x\,\partial\theta} + \frac{4}{15r}\frac{\partial^2 u_0}{\partial x\,\partial\theta} + \frac{4z}{15r}\frac{\partial^2\phi_x}{\partial x\,\partial\theta} \\ &\left.-\frac{1}{5r^2}\frac{\partial^2 v_0}{\partial\theta^2} - \frac{z}{5r^2}\frac{\partial^2\phi_\theta}{\partial\theta^2} - \frac{1}{5r^2}\frac{\partial w_0}{\partial\theta}\right),\end{aligned} \tag{20e}$$

$$\begin{aligned}&\tau_{xxz} = 2\mu l_1^2\eta_{xxz} = 2\mu l_1^2 \\ &\left(\frac{4}{15}\frac{\partial^2 w_0}{\partial x^2} + \frac{8}{15}\frac{\partial\phi_x}{\partial x} - \frac{1}{15r^2}\frac{\partial^2 w_0}{\partial\theta^2} - \frac{2}{15r}\frac{\partial\phi_\theta}{\partial\theta} + \frac{1}{15r^2}\frac{\partial v_0}{\partial\theta}\right),\end{aligned} \tag{20f}$$

$$\begin{aligned}\tau_{\theta\theta x} &= 2\mu l_1^2\eta_{\theta\theta x} = 2\mu l_1^2\left(\frac{4}{15r}\frac{\partial^2 v_0}{\partial x\,\partial\theta} + \frac{4}{15r}z\,\frac{\partial^2\phi_\theta}{\partial x\,\partial\theta}\right. \\ &+\frac{4}{15r^2}\frac{\partial^2 u_0}{\partial\theta^2} + \frac{4z}{15r^2}\frac{\partial^2\phi_x}{\partial\theta^2} + \frac{4}{15r}\frac{\partial^2 v_0}{\partial x\,\partial\theta} + \frac{4z}{15r}\frac{\partial^2\phi_\theta}{\partial x\,\partial\theta} \\ &\left.+\frac{4}{15r^2}\frac{\partial w_\theta}{\partial x} - \frac{2}{15}\frac{\partial^2 u_0}{\partial x^2} - \frac{2z}{15}\frac{\partial^2\phi_x}{\partial x^2}\right),\end{aligned} \tag{20g}$$

$$\begin{aligned}&\tau_{\theta\theta z} = 2\mu l_1^2\eta_{\theta\theta z} = 2\mu l_1^2 \\ &\left(\frac{4}{15r^2}\frac{\partial^2 w_0}{\partial\theta^2} + \frac{8}{15r}\frac{\partial\phi_\theta}{\partial\theta} - \frac{1}{15}\frac{\partial^2 w_0}{\partial x^2} - \frac{2}{15}\frac{\partial\phi_x}{\partial x} - \frac{4}{15r^2}\frac{\partial v_0}{\partial\theta}\right),\end{aligned} \tag{20h}$$

$$\tau_{zzx} = 2\mu l_1^2 \eta_{zzx} = 2\mu l_1^2 \left(-\frac{1}{5}\frac{\partial^2 u_0}{\partial x^2} - \frac{z}{5}\frac{\partial^2 \phi_x}{\partial x^2} - \frac{1}{15r}\frac{\partial^2 v_0}{\partial x \partial \theta} - \frac{z}{15r}\frac{\partial^2 \phi_\theta}{\partial x \partial \theta} - \frac{1}{15r}\frac{\partial w_0}{\partial x} - \frac{1}{15}\frac{\partial^2 v_0}{\partial x \partial \theta} - \frac{z}{15}\frac{\partial^2 \phi_\theta}{\partial x \partial \theta} - \frac{1}{15r}\frac{\partial^2 u_0}{\partial \theta^2} - \frac{z}{15r}\frac{\partial^2 \phi_x}{\partial \theta^2} \right), \tag{20i}$$

$$\tau_{zz\theta} = 2\mu l_1^2 \eta_{zz\theta} = 2\mu l_1^2 \left(-\frac{1}{5r^2}\frac{\partial^2 v_0}{\partial \theta^2} - \frac{z}{5r^2}\frac{\partial^2 \phi_\theta}{\partial \theta^2} - \frac{1}{5r^2}\frac{\partial w_0}{\partial \theta} - \frac{1}{15r}\frac{\partial^2 u_0}{\partial x \partial \theta} - \frac{z}{15r}\frac{\partial^2 \phi_x}{\partial x \partial \theta} - \frac{1}{15}\frac{\partial^2 v_0}{\partial x^2} - \frac{z}{15}\frac{\partial^2 \phi_\theta}{\partial x^2} - \frac{1}{15r}\frac{\partial^2 u_0}{\partial x \partial \theta} - \frac{z}{15r}\frac{\partial^2 \phi_x}{\partial x \partial \theta} \right), \tag{20j}$$

$$m_{xx} = 2\mu l_2^2 \chi_{xx} = \mu l_2^2 \left[\frac{1}{r}\frac{\partial v_0}{\partial x} + \frac{z}{r}\frac{\partial \phi_\theta}{\partial x} + \frac{\partial \phi_\theta}{\partial x} - \frac{1}{r}\frac{\partial^2 w_0}{\partial x \partial \theta} \right], \tag{21a}$$

$$m_{\theta\theta} = 2\mu l_2^2 \chi_{\theta\theta} = \frac{\mu l_2^2}{r} \left[\frac{\partial^2 w_0}{\partial x \partial \theta} - \frac{\partial \phi_x}{\partial \theta} - \frac{\partial v_0}{\partial x} - z\frac{\partial \phi_\theta}{\partial x} + \frac{1}{r}\frac{\partial u_0}{\partial \theta} + \frac{z}{r}\frac{\partial \phi_x}{\partial \theta} \right], \tag{21b}$$

$$m_{zz} = 2\mu l_2^2 \chi_{zz} = \mu l_2^2 \left[-\frac{\partial \phi_\theta}{\partial x} + \frac{1}{r}\frac{\partial \phi_x}{\partial \theta} \right], \tag{21c}$$

$$m_{x\theta} = 2\mu l_2^2 \chi_{x\theta} = \frac{\mu l_2^2}{2} \left[\frac{\partial^2 w_0}{\partial x^2} - \frac{\partial \phi_x}{\partial x} + \frac{1}{r^2}\frac{\partial v_0}{\partial \theta} - \frac{1}{r^2}\frac{\partial^2 w_0}{\partial \theta^2} + \frac{z}{r^2}\frac{\partial \phi_\theta}{\partial \theta} + \frac{1}{r}\frac{\partial \phi_\theta}{\partial \theta} \right], \tag{21d}$$

$$m_{xz} = 2\mu l_2^2 \chi_{xz} = \frac{\mu l_2^2}{2} \left[-\frac{\partial^2 v_0}{\partial x^2} - z\frac{\partial^2 \phi_\theta}{\partial x^2} + \frac{1}{r}\frac{\partial^2 u_0}{\partial x \partial \theta} + \frac{z}{r}\frac{\partial^2 \phi_x}{\partial x \partial \theta} + \frac{1}{r}\phi_\theta \right], \tag{21e}$$

$$m_{\theta z} = 2\mu l_2^2 \chi_{\theta z} = \frac{\mu l_2^2}{2} \left[-\frac{1}{r}\frac{\partial w_0}{\partial x} + \frac{1}{r}\phi_x - \frac{1}{r}\frac{\partial^2 v_0}{\partial x \partial \theta} - \frac{z}{r}\frac{\partial^2 \phi_\theta}{\partial x \partial \theta} + \frac{1}{r^2}\frac{\partial^2 u_0}{\partial \theta^2} + \frac{z}{r^2}\frac{\partial^2 \phi_x}{\partial \theta^2} \right]. \tag{21f}$$

Noted that in above equations, Yong modulus and poison's ratio of system can be calculated by Mori-Tanaka model which is explained in next section.

2.3 Mori-Tanaka Model and agglomeration effects

In this section, the effective modulus of the concrete column reinforced by CNTs is developed. Different methods are available to obtain the average properties of a composite. Due to its simplicity and accuracy even at high volume fractions of the inclusions, the Mori-Tanaka method (Shi and Feng 2004) is employed in this section. The matrix is assumed to be isotropic and elastic, with the Young's modulus E_m and the Poisson's ratio υ_m. The experimental results show that the assumption of uniform dispersion for CNTs in the matrix is not correct and the most of CNTs are bent and centralized in one area of the matrix. These regions with concentrated nanoparticles are assumed to have spherical shapes, and are considered as ‘‘inclusions’’ with different elastic properties from the surrounding material. The total volume V_r of nanoparticles can be divided into the following two parts (Mori and Tanaka 1973)

$$V_r = V_r^{inclusion} + V_r^{m}, \tag{22}$$

where $V_r^{inclusion}$ and V_r^{m} are the volumes of nanoparticles dispersed in the spherical inclusions and in the matrix, respectively. Introduce two parameters ξ and ζ describe the agglomeration of nanoparticles

$$\xi = \frac{V_{inclusion}}{V}, \tag{23}$$

$$\zeta = \frac{V_r^{inclusion}}{V_r}. \tag{24}$$

However, the average volume fraction c_r of nanoparticles in the composite is

$$C_r = \frac{V_r}{V}. \tag{25}$$

Assume that all the orientations of the nanoparticles are completely random. Hence, the effective bulk modulus (K) and effective shear modulus (G) may be written as

$$K = K_{out}\left[1 + \frac{\xi\left(\frac{K_{in}}{K_{out}} - 1\right)}{1 + \alpha(1-\xi)\left(\frac{K_{in}}{K_{out}} - 1\right)}\right] \tag{26}$$

$$G = G_{out}\left[1 + \frac{\xi\left(\frac{G_{in}}{G_{out}} - 1\right)}{1 + \beta(1-\xi)\left(\frac{G_{in}}{G_{out}} - 1\right)}\right], \tag{27}$$

where

$$K_{in} = K_m + \frac{(\delta_r - 3K_m\chi_r)C_r\zeta}{3(\xi - C_r\zeta + C_r\zeta\chi_r)}, \tag{28}$$

$$K_{out} = K_m + \frac{C_r\left(\delta_r - 3K_m\chi_r\right)\left(1-\zeta\right)}{3\left[1-\xi-C_r\left(1-\zeta\right)+C_r\chi_r\left(1-\zeta\right)\right]}, \quad (29)$$

$$G_{in} = G_m + \frac{\left(\eta_r - 3G_m\beta_r\right)C_r\zeta}{2\left(\xi - C_r\zeta + C_r\zeta\beta_r\right)}, \quad (30)$$

$$G_{out} = G_m + \frac{C_r\left(\eta_r - 3G_m\beta_r\right)\left(1-\zeta\right)}{2\left[1-\xi-C_r\left(1-\zeta\right)+C_r\beta_r\left(1-\zeta\right)\right]}, \quad (31)$$

where $\chi_r, \beta_r, \delta_r, \eta_r$ may be calculated as

$$\chi_r = \frac{3\left(K_m + G_m\right) + k_r - l_r}{3\left(k_r + G_m\right)}, \quad (32)$$

$$\beta_r = \frac{1}{5}\left\{\begin{array}{l} \frac{4G_m + 2k_r + l_r}{3\left(k_r + G_m\right)} + \frac{4G_m}{\left(p_r + G_m\right)} \\ + \frac{2\left[G_m\left(3K_m + G_m\right) + G_m\left(3K_m + 7G_m\right)\right]}{G_m\left(3K_m + G_m\right) + m_r\left(3K_m + 7G_m\right)} \end{array}\right\}, \quad (33)$$

$$\delta_r = \frac{1}{3}\left[n_r + 2l_r + \frac{\left(2k_r - l_r\right)\left(3K_m + 2G_m - l_r\right)}{k_r + G_m}\right], \quad (34)$$

$$\eta_r = \frac{1}{5}\left[\begin{array}{l} \frac{2}{3}\left(n_r - l_r\right) + \frac{4G_m p_r}{\left(p_r + G_m\right)} + \frac{2\left(k_r - l_r\right)\left(2G_m + l_r\right)}{3\left(k_r + G_m\right)} \\ + \frac{8G_m m_r\left(3K_m + 4G_m\right)}{3K_m\left(m_r + G_m\right) + G_m\left(7m_r + G_m\right)} \end{array}\right], \quad (35)$$

where k_r, l_r, n_r, p_r, m_r are the Hills elastic modulus for the CNTs [17]; K_m and G_m are the bulk and shear moduli of the matrix which can be written as

$$K_m = \frac{E_m}{3\left(1 - 2\upsilon_m\right)} \quad (36)$$

$$G_m = \frac{E_m}{2\left(1 + \upsilon_m\right)}. \quad (37)$$

Furthermore, β, α can be obtained from

$$\alpha = \frac{\left(1 + \upsilon_{out}\right)}{3\left(1 - \upsilon_{out}\right)} \quad (38)$$

$$\beta = \frac{2\left(4 - 5\upsilon_{out}\right)}{15\left(1 - \upsilon_{out}\right)}, \quad (39)$$

$$\upsilon_{out} = \frac{3K_{out} - 2G_{out}}{6K_{out} + 2G_{out}}. \quad (40)$$

Finally, the elastic modulus (E) and poison's ratio (υ) can be calculated as

$$E = \frac{9KG}{3K + G} \quad (41)$$

$$\upsilon = \frac{3K - 2G}{6K + 2G}. \quad (42)$$

2.4 Motion equations

Here, the energy method and Hamilton's principal are used. The potential energy can be calculated by Eq. (1). The kinetic energy of the structure is

$$K = \frac{1}{2}\int_{-\frac{h}{2}}^{\frac{h}{2}}\int_0^{2\pi}\int_0^{l}\rho\left[\left(\frac{\partial U}{\partial t}\right)^2 + \left(\frac{\partial V}{\partial t}\right)^2 + \left(\frac{\partial W}{\partial t}\right)^2\right]dx\,d\theta\,dz, \quad (43)$$

where ρ represents the density of structure.

The external work due to surrounding elastic medium is written as (Kolahchi *et al*. 2016a, b)

$$W = \int_0^{2\pi}\int_0^{L}\underbrace{\left(\begin{array}{l} -k_w w + G_\xi\left(\cos^2\theta w_{,xx} + 2\cos\theta\sin\theta w_{,yx} + \sin^2\theta w_{,yy}\right) \\ + G_\eta\left(\sin^2\theta w_{,xx} - 2\sin\theta\cos\theta w_{,yx} + \cos^2\theta w_{,yy}\right) \end{array}\right)}_{p} dA, \quad (44)$$

where θ describes the local ξ direction of orthotropic foundation with respect to the global x-axis of the shell; G_ξ and G_η are the shear constants in ξ and η directions, respectively; k_W is the spring constant.

The external work by the axial magnetic field can be expressed as (Kolahchi *et al*. 2016b)

$$W = \int\left(\underbrace{\eta h H_x^2\frac{\partial^2 w}{\partial x^2}}_{q}\right)w\,dA, \quad (45)$$

where η is the magnetic permeability of the CNTs and H_x is the magnetic field. Substituting expressions (1), (43), (44) and (45) into Hamilton's principle (i.e., $\int_0^t \delta\left(K - U + W\right)dt = 0$) and integrating by parts and setting the coefficients of mechanical displacements to zero, lead to the following motion equations

$$\begin{aligned} &\frac{\partial N_{xx}}{\partial x} + \frac{1}{r}\frac{\partial N_{x\theta}}{\partial\theta} - \frac{\partial^2 Y_x^0}{\partial x^2} - \frac{1}{r}\frac{\partial^2 Y_\theta^0}{\partial x\partial\theta} - \frac{2}{5}\frac{\partial^2 Y_{xxx}^1}{\partial x^2} \\ &+ \frac{1}{5r^2}\frac{\partial^2 Y_{xxx}^1}{\partial\theta^2} + \frac{2}{5r}\frac{\partial^2 Y_{\theta\theta\theta}^1}{\partial x\partial\theta} - \frac{8}{5r}\frac{\partial^2 Y_{xx\theta}^1}{\partial x\partial\theta} \\ &- \frac{4}{5r^2}\frac{\partial^2 Y_{\theta\theta x}^1}{\partial\theta^2} + \frac{3}{5}\frac{\partial^2 Y_{\theta\theta x}^1}{\partial x^2} + \frac{3}{5}\frac{\partial^2 Y_{zzx}^1}{\partial x^2} \\ &+ \frac{1}{5r^2}\frac{\partial^2 Y_{zzx}^1}{\partial\theta^2} + \frac{2}{5r}\frac{\partial^2 Y_{zz\theta}^1}{\partial x\partial\theta} + \frac{1}{2r^2}\frac{\partial^2 Y_{\theta\theta}^2}{\partial\theta} - \frac{1}{2r}\frac{\partial^2 Y_{xz}^2}{\partial x\partial\theta} \end{aligned} \quad (46)$$

$$-\frac{1}{2r^2}\frac{\partial^2 Y_{\theta z}^2}{\partial\theta^2}=I_1\frac{\partial^2 u_0}{\partial t^2}+I_2\frac{\partial^2\phi_x}{\partial t^2},$$

$$\begin{aligned}&\frac{1}{r}\frac{\partial N_{\theta\theta}}{\partial\theta}+\frac{\partial N_{x\theta}}{\partial x}+\frac{N_{\theta z}}{r}-\frac{1}{r}\frac{\partial^2 Y_x^0}{\partial x\partial\theta}-\frac{1}{r^2}\frac{\partial^2 Y_\theta^0}{\partial\theta^2}\\&+\frac{2}{5r}\frac{\partial^2 Y_{xxx}^1}{\partial x\partial\theta}-\frac{2}{5r^2}\frac{\partial^2 Y_{\theta\theta\theta}^1}{\partial\theta^2}+\frac{1}{5}\frac{\partial^2 Y_{\theta\theta\theta}^1}{\partial x^2}-\frac{4}{5}\frac{\partial^2 Y_{xx\theta}^1}{\partial x^2}\\&+\frac{3}{5r^2}\frac{\partial^2 Y_{xx\theta}^1}{\partial\theta^2}-\frac{8}{5r}\frac{\partial^2 Y_{\theta\theta x}^1}{\partial x\partial\theta}+\frac{2}{5r}\frac{\partial^2 Y_{zzx}^1}{\partial x\partial\theta}+\frac{3}{5r^2}\frac{\partial^2 Y_{zz\theta}^1}{\partial\theta^2}\\&+\frac{1}{5}\frac{\partial^2 Y_{zz\theta}^1}{\partial x^2}+\frac{1}{2r}\frac{\partial Y_{xx}^2}{\partial x}-\frac{1}{2r}\frac{\partial Y_{\theta\theta}^2}{\partial x}+\frac{1}{2r^2}\frac{\partial Y_{x\theta}^2}{\partial\theta}\\&+\frac{1}{2}\frac{\partial^2 Y_{xz}^2}{\partial x^2}+\frac{1}{2r}\frac{\partial^2 Y_{\theta z}^2}{\partial x\partial\theta}+\frac{1}{5r^2}\frac{\partial Y_{zzz}^1}{\partial\theta}-\frac{1}{r}\frac{\partial Y_{x\theta z}^1}{\partial x}\\&+\frac{1}{5r^2}\frac{\partial Y_{xxz}^1}{\partial\theta}-\frac{4}{5r^2}\frac{\partial Y_{\theta\theta z}^1}{\partial\theta}=I_1\frac{\partial^2 v_0}{\partial t^2}+I_2\frac{\partial^2\phi_\theta}{\partial t^2},\end{aligned}\tag{47}$$

$$\begin{aligned}&\frac{1}{2r}\frac{\partial^2 Y_{xx}^2}{\partial x\partial\theta}-\frac{1}{2r}\frac{\partial^2 Y_{\theta\theta}^2}{\partial x\partial\theta}-\frac{1}{2}\frac{\partial^2 Y_{x\theta}^2}{\partial x^2}\\&+\frac{1}{2r^2}\frac{\partial^2 Y_{x\theta}^2}{\partial\theta^2}-\frac{1}{2r}\frac{\partial Y_{\theta z}^2}{\partial x}+\frac{1}{5}\frac{\partial^2 Y_{zzz}^1}{\partial x^2}\\&+\frac{1}{5r^2}\frac{\partial^2 Y_{zzz}^2}{\partial\theta^2}-\frac{2}{r}\frac{\partial^2 Y_{x\theta z}^1}{\partial x\partial\theta}-\frac{3}{5r^2}\frac{\partial Y_{xx\theta}^1}{\partial\theta}\\&+\frac{1}{5r^2}\frac{\partial^2 Y_{xxz}^1}{\partial\theta^2}-\frac{4}{5}\frac{\partial^2 Y_{xxz}^1}{\partial x^2}+\frac{4}{5r}\frac{\partial Y_{\theta\theta x}^1}{\partial x}\\&-\frac{4}{5r^2}\frac{\partial^2 Y_{\theta\theta z}^1}{\partial\theta^2}+\frac{1}{5}\frac{\partial^2 Y_{\theta\theta z}^1}{\partial x^2}-\frac{1}{5r}\frac{\partial Y_{zzx}^1}{\partial x}\\&-\frac{3}{5r^2}\frac{\partial Y_{zz\theta}^1}{\partial\theta}-\frac{N_{\theta\theta}}{r}+\frac{\partial N_{xz}}{\partial x}\\&+\frac{1}{r}\frac{\partial N_{\theta z}}{\partial\theta}+\frac{1}{r}\frac{\partial Y_x^0}{\partial x}-\frac{1}{5r}\frac{\partial Y_{xxx}^1}{\partial x}\\&+\frac{2}{5r^2}\frac{\partial Y_{\theta\theta\theta}^1}{\partial\theta}+\frac{1}{r^2}\frac{\partial Y_\theta^0}{\partial\theta}+q+P=I_1\frac{\partial^2 w_0}{\partial t^2},\end{aligned}\tag{48}$$

$$\begin{aligned}&\frac{\partial M_{xx}}{\partial x}+\frac{1}{r}\frac{\partial M_{x\theta}}{\partial\theta}-N_{xz}-\frac{\partial^2 T_x^0}{\partial x^2}-\frac{1}{r}\frac{\partial^2 T_\theta^0}{\partial x\partial\theta}\\&+\frac{\partial Y_z^0}{\partial x}-\frac{2}{5}\frac{\partial^2 T_{xxx}^1}{\partial x^2}+\frac{1}{5r^2}\frac{\partial^2 T_{xxx}^1}{\partial\theta^2}\\&+\frac{2}{5r}\frac{\partial^2 T_{\theta\theta\theta}^1}{\partial x\partial\theta}-\frac{2}{5}\frac{\partial Y_{zzz}^1}{\partial x}+\frac{2}{r}\frac{\partial Y_{x\theta z}^1}{\partial\theta}\\&-\frac{8}{5r}\frac{\partial^2 T_{xx\theta}^1}{\partial x\partial\theta}+\frac{8}{5}\frac{\partial Y_{xxz}^1}{\partial x}-\frac{4}{5r^2}\frac{\partial^2 T_{\theta\theta x}^1}{\partial\theta^2}+\frac{3}{5}\frac{\partial^2 T_{\theta\theta x}^1}{\partial x^2}\\&-\frac{2}{5}\frac{\partial Y_{\theta\theta z}^1}{\partial x}+\frac{3}{5}\frac{\partial^2 T_{zzx}^1}{\partial x^2}+\frac{1}{5r^2}\frac{\partial^2 T_{zzx}^1}{\partial\theta^2}\\&+\frac{2}{5r}\frac{\partial^2 T_{zz\theta}^1}{\partial x\partial\theta}-\frac{1}{2r}\frac{\partial Y_{\theta\theta}^2}{\partial\theta}+\frac{1}{2r^2}\frac{\partial T_{\theta\theta}^2}{\partial\theta}\\&+\frac{1}{2r}\frac{\partial Y_{zz}^2}{\partial\theta}-\frac{1}{2}\frac{\partial Y_{x\theta}^2}{\partial x}-\frac{1}{2r}\frac{\partial^2 T_{xz}^2}{\partial x\partial\theta}-\frac{1}{2r}Y_{\theta z}^2\\&-\frac{1}{2r^2}\frac{\partial^2 T_{\theta z}^2}{\partial\theta^2}=I_2\frac{\partial^2 u_0}{\partial t^2}+I_3\frac{\partial^2\phi_x}{\partial t^2},\end{aligned}\tag{49}$$

$$\begin{aligned}&\frac{1}{r}\frac{\partial M_{\theta\theta}}{\partial\theta}+\frac{\partial M_{x\theta}}{\partial x}-N_{\theta z}+\frac{M_{\theta z}}{r}-\frac{1}{r}\frac{\partial^2 T_x^0}{\partial x\partial\theta}\\&-\frac{1}{r^2}\frac{\partial^2 T_\theta^0}{\partial\theta^2}+\frac{1}{r}\frac{\partial Y_z^0}{\partial\theta}+\frac{2}{5r}\frac{\partial^2 T_{xxx}^1}{\partial x\partial\theta}-\\&\frac{2}{5r^2}\frac{\partial^2 T_{\theta\theta\theta}^1}{\partial\theta^2}+\frac{1}{5}\frac{\partial^2 T_{\theta\theta\theta}^1}{\partial x^2}-\frac{2}{5r}\frac{\partial Y_{zzz}^1}{\partial\theta}\\&+2\frac{\partial Y_{x\theta z}^1}{\partial x}+\frac{1}{5r^2}\frac{\partial^2 T_{zzz}^1}{\partial\theta}-\frac{4}{5}\frac{\partial^2 T_{xx\theta}^1}{\partial x^2}\\&-\frac{1}{r}\frac{\partial T_{x\theta z}^1}{\partial x}+\frac{3}{5r^2}\frac{\partial^2 T_{xx\theta}^1}{\partial\theta^2}-\frac{2}{5r}\frac{\partial Y_{xxz}^1}{\partial\theta}\\&+\frac{1}{5r^2}\frac{\partial T_{xxz}^1}{\partial\theta}-\frac{8}{5r}\frac{\partial^2 T_{\theta\theta x}^1}{\partial x\partial\theta}+\frac{8}{5r}\frac{\partial Y_{\theta\theta z}^1}{\partial\theta}\\&-\frac{4}{5r^2}\frac{\partial T_{\theta\theta z}^1}{\partial\theta}+\frac{2}{5r}\frac{\partial^2 T_{zzx}^1}{\partial x\partial\theta}+\frac{3}{5r^2}\frac{\partial^2 T_{zz\theta}^1}{\partial\theta^2}\\&+\frac{1}{5}\frac{\partial^2 T_{zz\theta}^1}{\partial x^2}+\frac{1}{2r}\frac{\partial T_{xx}^2}{\partial x}-\frac{Y_{zz\theta}^1}{5r}+\frac{1}{2}\frac{\partial Y_{xx}^2}{\partial x}\\&-\frac{1}{2r}\frac{\partial T_{\theta\theta}^2}{\partial x}-\frac{1}{2}\frac{\partial Y_{zz}^2}{\partial x}+\frac{1}{2r^2}\frac{\partial T_{x\theta}^2}{\partial\theta}\\&+\frac{1}{2r}\frac{\partial Y_{x\theta}^2}{\partial\theta}+\frac{1}{2}\frac{\partial^2 T_{xz}^2}{\partial x^2}-\frac{Y_{xz}^2}{2r}+\frac{1}{2r}\frac{\partial^2 T_{\theta z}^2}{\partial x\partial\theta}\\&=I_2\frac{\partial^2 v_0}{\partial t^2}+I_3\frac{\partial^2\phi_\theta}{\partial t^2},\end{aligned}\tag{50}$$

In above equations, the moment of inertia can be defined as

$$\left(I_1,I_2,I_3\right)=\int_{-\frac{h}{2}}^{\frac{h}{2}}\rho\left(1,z,z^2\right)dz.\tag{51}$$

In addition, the stress resultant can be expressed as follows

$$
\begin{aligned}
&N_{ij}=\int_{-\frac{h}{2}}^{\frac{h}{2}}\sigma_{ij}dz\,, \qquad M_{ij}=\int_{-\frac{h}{2}}^{\frac{h}{2}}\sigma_{ij}zdz\,,\\
&Y_{ij}^{(2)}=\int_{-\frac{h}{2}}^{\frac{h}{2}}m_{ij}^{s}dz\,, \qquad T_{ij}^{(2)}=\int_{-\frac{h}{2}}^{\frac{h}{2}}m_{ij}^{s}zdz\,,\\
&Y_{ijk}^{(1)}=\int_{-\frac{h}{2}}^{\frac{h}{2}}\tau_{ijk}^{1}dz\,, \qquad T_{ijk}^{(1)}=\int_{-\frac{h}{2}}^{\frac{h}{2}}\tau_{ijk}^{1}zdz\,,\\
&Y_{i}^{(0)}=\int_{-\frac{h}{2}}^{\frac{h}{2}}P_{i}dz\,, \qquad T_{i}^{(0)}=\int_{-\frac{h}{2}}^{\frac{h}{2}}P_{i}zdz\,.
\end{aligned}
\tag{52}
$$

Substituting Eqs. (18)-(21) into Eq. (52) yields

$$N_{xx}=\frac{Eh}{1-\nu^{2}}\left(\frac{\partial U}{\partial x}+\nu\frac{W}{r}\right), \tag{53a}$$

$$N_{\theta\theta}=\frac{Eh}{1-\nu^{2}}\left(\frac{W}{r}+\nu\frac{\partial U}{\partial x}\right), \tag{53b}$$

$$N_{x\theta}=\mu h\left(\frac{1}{r}\frac{\partial U}{\partial\theta}+\frac{\partial V}{\partial x}\right), \tag{53c}$$

$$N_{xz}=\mu h\left(\Phi_{x}+\frac{\partial W}{\partial x}\right), \tag{53d}$$

$$N_{\theta z}=\mu h\left(\frac{1}{r}\frac{\partial W}{\partial\theta}+\Phi_{\theta}-\frac{V}{r}\right), \tag{53e}$$

$$M_{xx}=\frac{1}{12}\frac{Eh^{3}}{1-\nu^{2}}\left(\frac{\partial\Phi_{x}}{\partial x}+\frac{\nu}{r}\frac{\partial\Phi_{\theta}}{\partial\theta}\right), \tag{54a}$$

$$M_{\theta\theta}=\frac{1}{12}\frac{Eh^{3}}{1-\nu^{2}}\left(\nu\frac{\partial\Phi_{x}}{\partial x}+\frac{1}{r}\frac{\partial\Phi_{\theta}}{\partial\theta}\right), \tag{54b}$$

$$M_{x\theta}=\frac{1}{12}\mu h^{3}\left(\frac{\partial\Phi_{\theta}}{\partial x}+\frac{1}{r}\frac{\partial\Phi_{x}}{\partial\theta}\right), \tag{54c}$$

$$Y_{x}^{0}=2\mu l_{0}^{2}h\left(\frac{\partial^{2}U}{\partial x^{2}}+\frac{1}{r}\frac{\partial W}{\partial x}\right), \tag{55a}$$

$$Y_{\theta}^{0}=2\mu l_{0}^{2}h\left(\frac{1}{r}\frac{\partial^{2}U}{\partial x\partial\theta}+\frac{1}{r^{2}}\frac{\partial W}{\partial\theta}\right), \tag{55b}$$

$$Y_{z}^{0}=2\mu l_{0}^{2}h\left(\frac{\partial\Phi_{x}}{\partial x}+\frac{1}{r}\frac{\partial\Phi_{\theta}}{\partial\theta}\right), \tag{55c}$$

$$Y_{xxx}^{1}=\frac{2}{5}\mu l_{1}^{2}h\left(2\frac{\partial^{2}U}{\partial x^{2}}-\frac{1}{r}\frac{\partial W}{\partial x}-\frac{1}{r^{2}}\frac{\partial^{2}U}{\partial\theta^{2}}\right), \tag{56d}$$

$$Y_{\theta\theta\theta}^{1}=\frac{2}{5}\mu l_{1}^{2}h\left(\frac{2}{r^{2}}\frac{\partial W}{\partial\theta}-\frac{2}{r}\frac{\partial^{2}U}{\partial x\partial\theta}-\frac{\partial^{2}V}{\partial x^{2}}\right), \tag{56e}$$

$$Y_{zzz}^{1}=\frac{2}{5}\mu l_{1}^{2}h\left(-2\frac{\partial\Phi_{x}}{\partial x}-\frac{2}{r}\frac{\partial\Phi_{\theta}}{\partial\theta}-\frac{\partial^{2}W}{\partial x^{2}}-\frac{1}{r^{2}}\frac{\partial^{2}W}{\partial\theta^{2}}\right), \tag{56f}$$

$$Y_{xx\theta}^{1}=\frac{2}{15}\mu l_{1}^{2}h\left(4\frac{\partial^{2}V}{\partial x^{2}}+\frac{8}{r}\frac{\partial^{2}U}{\partial x\partial\infty}-\frac{3}{r^{2}}\frac{\partial W}{\partial\theta}\right), \tag{56g}$$

$$Y_{xxz}^{1}=\frac{2}{15}\mu l_{1}^{2}h\left(4\frac{\partial^{2}W}{\partial x^{2}}+8\frac{\partial\Phi_{x}}{\partial x}-\frac{2}{r}\frac{\partial\Phi_{\theta}}{\partial\theta}-\frac{1}{r}\frac{\partial^{2}W}{\partial\theta^{2}}\right), \tag{56h}$$

$$Y_{\theta\theta x}^{1}=\frac{2}{15}\mu l_{1}^{2}h\left(\frac{4}{r^{2}}\frac{\partial^{2}U}{\partial\theta^{2}}+\frac{4}{r}\frac{\partial W}{\partial x}-3\frac{\partial^{2}U}{\partial x^{2}}\right), \tag{56i}$$

$$Y_{\theta\theta z}^{1}=\frac{2}{15}\mu l_{1}^{2}h\left(\frac{4}{r^{2}}\frac{\partial^{2}W}{\partial\theta^{2}}+\frac{8}{r}\frac{\partial\Phi_{\theta}}{\partial\theta}-\frac{2}{15}\frac{\partial\Phi_{x}}{\partial x}-\frac{1}{15}\frac{\partial^{2}W}{\partial x^{2}}\right), \tag{56j}$$

$$Y_{zzx}^{1}=\frac{2}{15}\mu l_{1}^{2}h\left(-3\frac{\partial^{2}U}{\partial x^{2}}-\frac{1}{r}\frac{\partial W}{\partial x}-\frac{1}{15r^{2}}\frac{\partial^{2}U}{\partial\theta^{2}}\right), \tag{56k}$$

$$Y_{zz\theta}^{1}=\frac{2}{15}\mu l_{1}^{2}h\left(-\frac{2}{r}\frac{\partial^{2}U}{\partial x\partial\theta}-\frac{3}{r^{2}}\frac{\partial W}{\partial\theta}-\frac{\partial^{2}V}{\partial x^{2}}\right), \tag{56l}$$

$$Y_{x\theta z}^{1}=\frac{1}{3}\mu l_{1}^{2}h\left(\frac{2}{r}\frac{\partial^{2}W}{\partial x\partial\theta}+2\frac{\partial\Phi_{\theta}}{\partial x}-\frac{1}{r}\frac{\partial V}{\partial x}+\frac{2}{r}\frac{\partial\Phi_{x}}{\partial\theta}\right), \tag{56m}$$

$$Y_{xx}^{2}=\mu l_{2}^{2}h\left(\frac{1}{r}\frac{\partial V}{\partial x}+\frac{\partial\Phi_{\theta}}{\partial x}-\frac{1}{r}\frac{\partial^{2}W}{\partial x\partial\theta}\right), \tag{57a}$$

$$Y_{\theta\theta}^{2}=\mu l_{2}^{2}h\left(\frac{1}{r}\frac{\partial^{2}W}{\partial x^{2}}-\frac{1}{r}\frac{\partial\Phi_{x}}{\partial\theta}-\frac{1}{r}\frac{\partial V}{\partial x}+\frac{1}{r^{2}}\frac{\partial U}{\partial\theta}\right), \tag{57b}$$

$$Y_{zz}^{2}=\mu l_{2}^{2}h\left(\frac{1}{r}\frac{\partial\Phi_{x}}{\partial\theta}-\frac{\partial\Phi_{\theta}}{\partial x}\right), \tag{57c}$$

$$Y_{x\theta}^{2}=\frac{1}{2}\mu l_{2}^{2}h\left(\frac{\partial^{2}W}{\partial x^{2}}-\frac{\partial\Phi_{x}}{\partial x}-\frac{1}{r^{2}}\frac{\partial^{2}W}{\partial\theta^{2}}+\frac{1}{r}\frac{\partial\Phi_{\theta}}{\partial\theta}\right), \tag{57d}$$

$$Y_{xz}^{2}=\frac{1}{2}\mu l_2^2 h\left(-\frac{\partial^2 V}{\partial x^2}+\frac{1}{r}\frac{\partial^2 U}{\partial x\partial\theta}+\frac{1}{r}\Phi_\theta\right), \quad (57e)$$

$$Y_{\theta z}^{2}=\frac{1}{2}\mu l_2^2 h\left(-\frac{1}{r}\frac{\partial W}{\partial x}+\frac{1}{r}\Phi_x+\frac{1}{r^2}\frac{\partial^2 U}{\partial\theta^2}\right), \quad (57f)$$

$$T_x^{0}=\frac{1}{6}\mu l_0^2 h^3\left(\frac{\partial^2\Phi_x}{\partial x^2}+\frac{1}{r}\frac{\partial^2\Phi_\theta}{\partial x\partial\theta}\right), \quad (58a)$$

$$T_\theta^{0}=\frac{1}{6}\mu l_0^2 h^3\left(\frac{1}{r}\frac{\partial^2\Phi_x}{\partial x^2}+\frac{1}{r^2}\frac{\partial^2\Phi_\theta}{\partial x\partial\theta}\right), \quad (58b)$$

$$T_z^{0}=0, \quad (58c)$$

$$T_{xxx}^{1}=\frac{1}{30}\mu l_1^2 h^3\left(2\frac{\partial^2\Phi_x}{\partial x^2}-\frac{2}{r}\frac{\partial^2\Phi_\theta}{\partial x\partial\theta}-\frac{1}{r^2}\frac{\partial^2\Phi_x}{\partial\theta^2}\right), \quad (59a)$$

$$T_{\theta\theta\theta}^{1}=\frac{1}{30}\mu l_1^2 h^3\left(\frac{2}{r^2}\frac{\partial^2\Phi_\theta}{\partial\theta^2}-\frac{2}{r}\frac{\partial^2\Phi_x}{\partial x\partial\theta}-\frac{\partial^2\Phi_\theta}{\partial x^2}\right), \quad (59b)$$

$$T_{zzz}^{1}=0, \quad (59c)$$

$$T_{xx\theta}^{1}=\frac{1}{90}\mu l_1^2 h^3\left(4\frac{\partial^2\Phi_\theta}{\partial x^2}+\frac{8}{r}\frac{\partial^2\Phi_x}{\partial x\partial\theta}-\frac{3}{r^2}\frac{\partial^2\Phi_\theta}{\partial\theta^2}\right), \quad (59d)$$

$$T_{xxz}^{1}=0, \quad (59e)$$

$$T_{\theta\theta x}^{1}=\frac{1}{90}\mu l_1^2 h^3\left(\frac{8}{r}\frac{\partial^2\Phi_\theta}{\partial x\partial\theta}+\frac{4}{r}\frac{\partial^2\Phi_x}{\partial\theta^2}-3\frac{\partial^2\Phi_x}{\partial x^2}\right), \quad (59f)$$

$$T_{\theta\theta z}^{1}=0, \quad (59g)$$

$$T_{zzx}^{1}=\frac{1}{30}\mu l_1^2 h^3\left(-3\frac{\partial^2\Phi_x}{\partial x^2}-\frac{2}{r}\frac{\partial^2\Phi_\theta}{\partial x\partial\theta}-\frac{1}{r^2}\frac{\partial^2\Phi_x}{\partial\theta^2}\right), \quad (59h)$$

$$T_{zz\theta}^{1}=\frac{1}{30}\mu l_1^2 h^3\left(-\frac{2}{r}\frac{\partial^2\Phi_x}{\partial x\partial\theta}-\frac{3}{r^2}\frac{\partial^2\Phi_\theta}{\partial\theta^2}-\frac{\partial^2\Phi_\theta}{\partial x^2}\right), \quad (59i)$$

$$T_{x\theta z}^{1}=0, \quad (59j)$$

$$T_{xx}^{2}=\frac{1}{12}\frac{\mu l_2^2 h^3}{r}\left(\frac{\partial\Phi_\theta}{\partial x}\right), \quad (60a)$$

$$T_{\theta\theta}^{2}=\frac{1}{12}\frac{\mu l_2^2 h^3}{r}\left(-\frac{\partial\Phi_\theta}{\partial x}+\frac{1}{r}\frac{\partial\Phi_x}{\partial\theta}\right), \quad (60b)$$

$$T_{zz}^{2}=0, \quad (60c)$$

$$T_{x\theta}^{2}=\frac{1}{24}\frac{\mu l_2^2 h^3}{r^2}\left(\frac{\partial\Phi_\theta}{\partial\theta}\right), \quad (60d)$$

$$T_{xz}^{2}=\frac{1}{24}\frac{\mu l_2^2 h^3}{r}\left(-\frac{\partial^2\Phi_x}{\partial x^2}+\frac{1}{r}\frac{\partial^2\Phi_x}{\partial x\partial\theta}\right). \quad (60e)$$

Noted that in the motion equations, ignoring l_0 and l_1 leads to the motion equations for the MCST. In addition, ignoring l_0, l_1 and l_2 leads to the motion equations for the classical cylindrical shell theory. In this paper, three types of boundary conditions are considered as follows

- **Simple-Simple (SS)**

$$x=0,L\Rightarrow u=v=w=\phi_\theta=M_{xx}=0, \quad (61)$$

- **Clamped- Clamped (CC)**

$$x=0,L\Rightarrow u=v=w=\phi_x=\phi_\theta=0, \quad (62)$$

- **Clamped- Simple (CS)**

$$\begin{aligned}&x=0\Rightarrow u=v=w=\phi_x=\phi_\theta=0,\\&x=L\Rightarrow u=v=w=\phi_x=M_{xx}=0.\end{aligned} \quad (63)$$

3. Solution procedure

At the first, the mechanical displacement of structure can be defined as (Ghorbanpour Arani *et al*. 2012)

$$u_o(x,\theta,t)=\sum_n u_n(\mathrm{x})\cos(\mathrm{n}\,\theta)e^{i\omega t}, \quad (64a)$$

$$v_o(x,\theta,t)=\sum_n v_n(\mathrm{x})\sin(\mathrm{n}\,\theta)e^{i\omega t}, \quad (64b)$$

$$w_o(x,\theta,t)=\sum_n w_n(\mathrm{x})\cos(\mathrm{n}\,\theta)e^{i\omega t}, \quad (64c)$$

$$\phi_x(x,\theta,t)=\sum_n \phi x_n(\mathrm{x})\cos(\mathrm{n}\,\theta)e^{i\omega t}, \quad (64d)$$

$$\phi_\theta(x,\theta,t)=\sum_n \phi\theta_n(\mathrm{x})\sin(\mathrm{n}\,\theta)e^{i\omega t}, \quad (64e)$$

where n is the circumferential wave number and ω is the frequency of structure. Substituting above equations into

Eqs. (46)-(50) and combine with Eqs. (53)-(60) leads to the differential motion equations in x direction. However, DQM is used for discretization of motion equations using following relation (Kolahchi *et al*. 2016a, b)

$$\frac{d^m f_x(x_i)}{dx^m} = \sum_{k=1}^{N_x} A_{ik}^{(m)} f(x_k) \qquad m = 1, \ldots, N_x - 1, \quad (65)$$

where N_x and $A_{ik}^{(m)}$ are the axial grid point number and weighting coefficient which may be defined as

$$x_i = \frac{L}{2}\left[1 - \cos\left(\frac{i-1}{N_x - 1}\right)\pi\right] \quad i = 1, \ldots, N_x, \qquad (66)$$

$$A_{ij}^{(1)} = \begin{cases} \dfrac{M(x_i)}{(x_i - x_j)M(x_j)} & for \quad i \neq j, \quad i, j = 1, 2, \ldots, N_x \\ -\sum\limits_{\substack{j=1 \\ i \neq j}}^{N_x} A_{ij}^{(1)} & for \quad i = j, \quad i, j = 1, 2, \ldots, N_x \end{cases} \qquad (67)$$

where

$$M(x_i) = \prod_{\substack{j=1 \\ j \neq i}}^{N_x} (x_i - x_j). \qquad (68)$$

For higher order derivatives we have

$$A_{ij}^{(m)} = m\left(A_{ii}^{(m-1)} A_{ij}^{(1)} - \frac{A_{ij}^{(m-1)}}{(x_i - x_j)}\right). \qquad (69)$$

Finally, the motion equations in matrix form can be expressed as

$$\{[K] - \omega^2 [M]\}\{d\} = [0], \qquad (70)$$

where $[d] = [u_n \; v_n \; w_n \; \phi x_n \; \phi\theta_n]^T$ is displacement amplitude vector. However, using an eigenvalue problem solution, the frequency of structure can be calculated.

4. Numerical results and discussion

A micro cylindrical shell with length to radius ratio (L/R=3) and thickness to radius ratio of (h/R=0.1) is considered which is made from polystyrene with the Yong modulus of E_m=1190 MPa and poison's ratio of v_m=0.3 is considered (Qian *et al*. 2000). The structure is reinforced with CNTs with the Hills elastic modulus reported in (Shi and Feng 2004). The small scale parameters are considered $l_0 = l_1 = l_2 = 17.6\ \mu m$. This section is divided to three parts including validation of present work, convergence and accuracy of DQM and discussing about the effects of different parameters on the dimensionless frequency ($\Omega = \omega R\sqrt{\rho / E}$) of structure.

4.1 Validation

Table 1 Validation of this work with Ref. [23]

h/R	*n*	Classical theory, Tadi Beni *et al*. (2014)	MCST, Tadi Beni *et al*. (2014)	Classical theory, Present work	MCST, Present work
0.1	1	0.933	1.126	0.9335	1.1264
	2	0.776	1.0688	0.7764	1.0688
	3	0.713	1.207	0.7132	1.2071
0.2	1	1.048	1.537	1.0483	1.5373
	2	0.971	1.590	0.9714	1.5901
	3	1.052	1.928	1.0522	1.9284
0.3	1	1.181	1.878	1.1812	1.8787
	2	1.162	1.974	1.1626	1.9742
	3	1.330	2.415	1.3305	2.4153

In order to validate the presented results, the elastic medium, magnetic field, l_0 and l_1 are ignored. However, the vibration of a nano cylindrical shell with Yong modulus of E=1.06 TPa, Poisson's ratio of v=0.3, radius of R=2 nm, density of ρ=2300 kg/m^3 and length to radius ratio of L/R=1 is considered. The size effects are considered based on MCST. The dimensionless frequency for different thickness to radius ratio (h/R) and circumferential wave number is reported in Table 1. The presented results based on DQM are compared with those reported by Tadi Beni *et al*. (2014). As can be seen, there are a good agreement between the results of this work and Tadi Beni *et al*. (2014).

4.2 DQM convergence

The effect of the grid point number in DQM on the dimensionless frequency of the structure is demonstrated in Fig. 2. As can be seen, fast rate of convergence of the method are quite evident and it is found that 14 DQM grid points can yield accurate results. However, in the present work, the number of grid point is selected to be 14 for obtaining the accurate results.

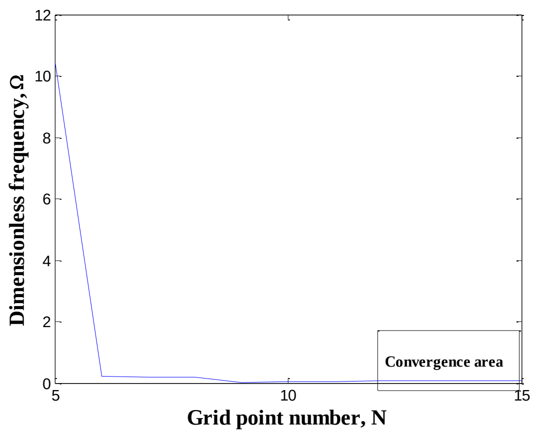

Fig. 2 The effect of DQ grid points number on the dimensionless frequency

4.3 The effects of different parameters

In Fig. 3, the first dimensionless frequency predicted by three theories of classical, MCST and SGT is plotted versus volume percent of CNTs for SS boundary condition. It can be seen that with increasing the volume percent of CNTs, the dimensionless frequency increases. It is due to the fact that with increasing the volume percent of CNTs, the stiffness of structure enhances. The dimensionless frequency obtained by the SGT is higher than that predicted by MCST. This is because the SGT expresses the three additional dilatation gradient tensor, the deviatoric stretch gradient tensor and the rotation gradient tensor while the MCST considered only the rotation gradient tensor. This figure illustrates that small scale theories, SGT and MCST have more difference with classical theory at higher volume percent of CNTs.

Size effects in SGT on the dimensionless frequency are shown in Fig. 4 as a function of CNTs volume percent. It is obvious that with increasing the small scale parameter, the dimensionless frequency of structure is enhanced. It is because with increasing the small scale parameter in the SGT, the stability of structure improved.

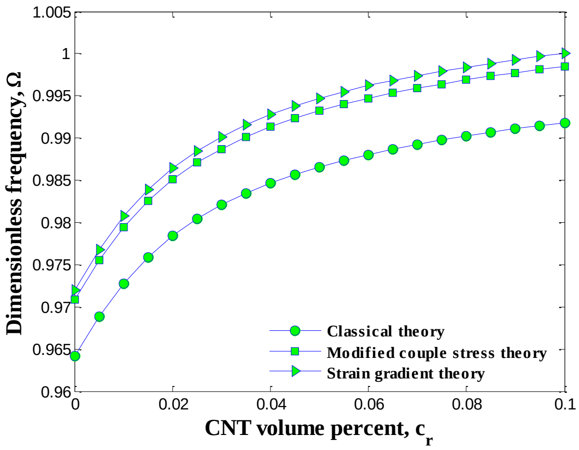

Fig. 3 Comparison of SGT, MCST and classical theory on the dimensionless frequency versus CNTs volume percent

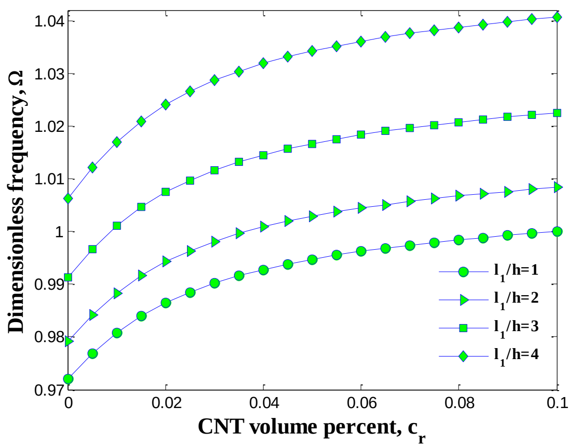

Fig. 4 The effect of material length scale parameter on the dimensionless frequency versus CNTs volume percent

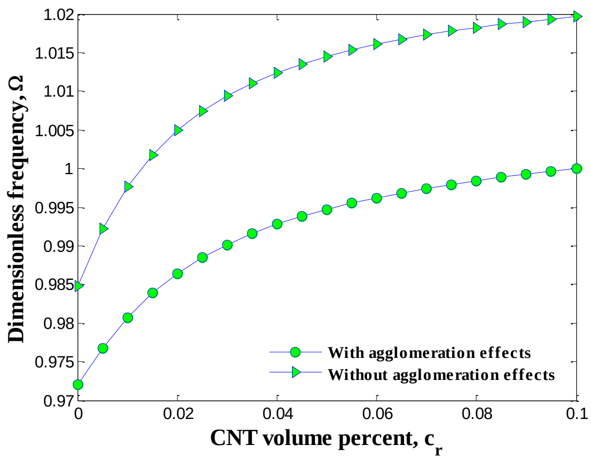

Fig. 5 The effect of CNT agglomeration on the dimensionless frequency versus CNTs volume percent

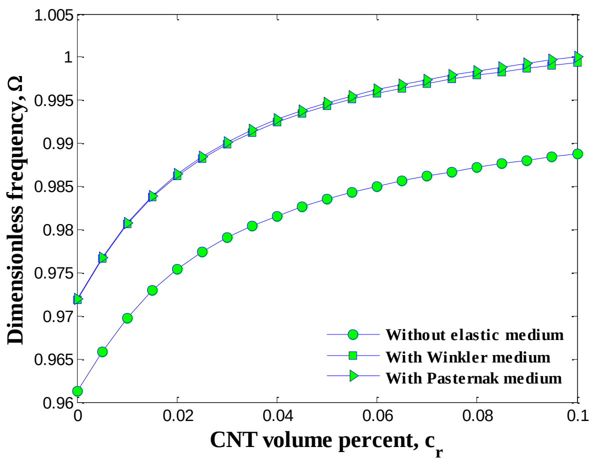

Fig. 6 The effect of elastic medium on the dimensionless frequency versus CNTs volume percent

The effects of agglomeration (ξ) on the dimensionless frequency versus volume percent of CNTs are demonstrated in Fig. 5. It is worth noting that the dimensionless frequency decreases with considering ξ. It is due to the fact that considering agglomeration effect leads to lower stiffness in structure. However, the agglomeration effect has a major effect on the vibration behaviour of the structure. In addition, with increasing the volume percent of CNTs, the dimensionless frequency is increased and the effect of agglomeration becomes more prominent.

Fig. 6 illustrates the effect of the elastic medium on the dimensionless frequency versus the CNTs volume percent for SGT. It can be found that considering elastic medium leads to more stiffness in the structure and consequently higher dimensionless frequency. Comparing Winkler-type and orthotropic Pasternak-type elastic medium, it is found that the dimensionless frequency predicted by the Pasternak medium is higher than that obtained by the Winkler medium. It is perhaps due to the fact that the Winkler-type is capable to describe just normal load of the elastic medium while the Pasternak-type describes both transverse shear and normal loads of the elastic medium.

In order to show the effect of magnetic field, Fig. 7 is

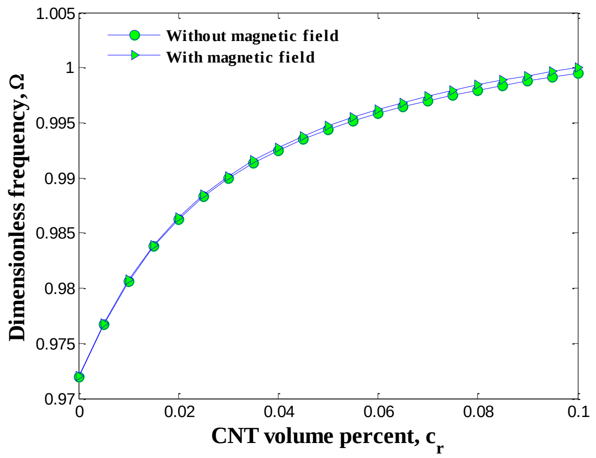

Fig. 7 The effect of magnetic field on the dimensionless frequency versus CNTs volume percent

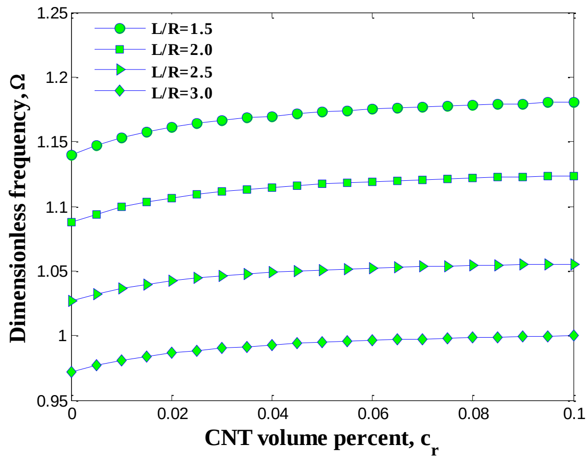

Fig. 9 The effect of length to radius ratio on the dimensionless frequency versus CNTs volume percent

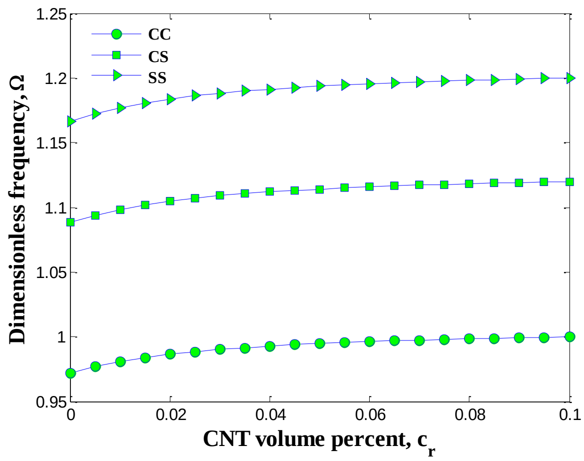

Fig. 8 The effect of boundary condition on the dimensionless frequency versus CNTs volume percent

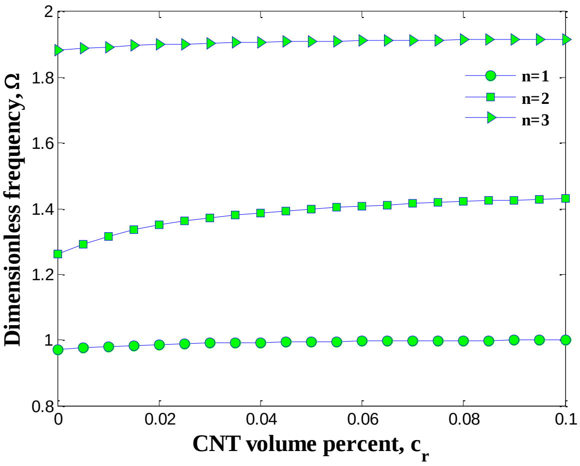

Fig. 10 The effect of circumferential wave number on the dimensionless frequency versus CNTs volume percent

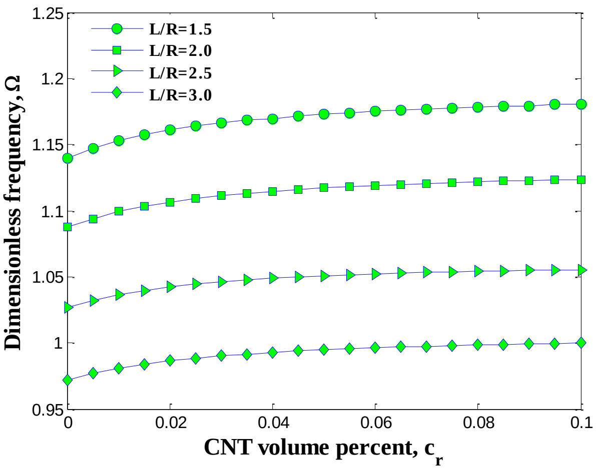

Fig. 9 The effect of length to radius ratio on the dimensionless frequency versus CNTs volume percent

presented. In this figure, the dimensionless frequency is plotted versus CNTs volume percent. It can be seen that considering magnetic field leads to higher dimensionless frequency due to increase in the stiffness of structure. Noted that the effect of magnetic field becomes more considerable with increasing CNTs volume percent.

The effect of the different boundary conditions on the dimensionless frequency of structure versus CNTs volume percent is illustrated in Fig. 8. It can be found that the dimensionless frequency predicted by CC cylindrical shell is higher with respect to other considered boundary conditions. It is because that considering CC boundary condition leads to harder structure.

The effect of circumferential wave number on the dimensionless frequency versus CNTs volume percent is shown in Fig. 9 considering agglomeration effects. Obviously, increasing the circumferential wave number leads to higher dimensionless frequency.

Fig. 10 demonstrates the effect of length to radius ratio of cylindrical shell on the dimensionless frequency against CNTs volume percent. As can be seen, with increasing the length to radius ratio, the dimensionless frequency is decreased due to the reduction in the stiffness of structure. In addition, in all length to radius ratios, the dimensionless frequency increases with increasing the CNTs volume percent.

5. Conclusions

Agglomeration effect on the vibration analysis of a micro cylindrical shell reinforced with CNTs was the main contribution of this work. The structure was simulated with Mindlin cylindrical shell theory mathematically. The characteristics of the equivalent composite were determined using Mori-Tanaka model. The structure was surrounded by orthotropic Pasternak medium and was subjected to axial magnetic field. Applying DQM, the frequency of structure was obtained and the effects of CNTs volume percent, agglomeration of CNTs, elastic medium, magnetic field, boundary conditions, length to radius ratio, circumferential wave number and small scale parameter were shown. Results indicate that with increasing the volume percent of CNTs, the frequency increases. It was also worth to mention that the frequency of micro cylindrical shell decreases considering agglomeration effects. Obviously, considering elastic medium and magnetic field as well as decreasing the length to radius ration lead to higher frequency. In addition, the frequency predicted by SGT was higher than those obtained by the MCST and classical theory. The results of this work were validated as far as possible with Tadi Beni *et al*. (2014). Finally, it is hoped that the results presented in this paper would be helpful for design and analysis of micro structures based cylindrical shell.

References

Akgoz, B. and Civalek, O. (2013), "Buckling analysis of linearly tapered micro-columns based on strain gradient elasticity", *Struct. Eng. Mech*., **48**(2), 195-205.

Alibeigloo, A. (2014), "Free vibration analysis of functionally graded carbon nanotube reinforced composite cylindrical panel embedded in piezoelectric layers by using theory of elasticity", *Eur. J. Mech. A/Solids*, **44**, 104-115.

Ansari, R., Gholami, R. and Norouzzadeh, A. (2016), "Size-dependent thermo-mechanical vibration and instability of conveying fluid functionally graded nanoshells based on Mindlin's strain gradient theory", *Thin-Wall. Struct*., **105**, 172-184.

Ayatollahi, M.R., Naeemi A.R. and Alishahi, E. (2015), "Effects of mixed contents of carbon nanoreinforcements on the impact resistance of epoxy-based nanocomposites", *Struct. Eng. Mech*., **56**(2), 157-167.

Changcheng, D. and Yinghui, L. (2013), "Nonlinear resonance behavior of functionally graded cylindrical shells in thermal environments", *Compos. Struct*., **102**, 164-174.

Civalek, E. (2016), "Free vibration of carbon nanotubes reinforced (CNTR) and functionally graded shells and plates based on FSDT via discrete singular convolution method", *Compos. Part B*, **111**, 45-59.

Gharib, A., Karimi, M.S. and Ghorbanpour Arani, A. (2016), "Vibration analysis of the embedded piezoelectric polymeric nano-composite panels in the elastic substrate", *Compos. Part B*, **101**, 64-76.

Gholami, R., Darvizeh, A., Ansari, R. and Sadeghi, F. (2016), "Vibration and buckling of first-order shear deformable circular cylindrical micro-/nano-shells based on Mindlin's strain gradient elasticity theory", *Eur. J. Mech. A/Solids*, **58**, 76-88.

Ghorbanpour Arani, A., Kolahchi, R. and Vossough, H. (2012), "Nonlocal wave propagation in an embedded DWBNNT conveying fluid via strain gradient theory", *Physica B*, **407**(21), 4281-4286.

Guo, S., He, Y., Liu, D., Lei, J., Shen, L. and Li, Zh. (2016), "Torsional vibration of carbon nanotube with axial velocity and velocity gradient effect", *Int. J. Mech. Sci.*, **119**, 88-96.

Iijima, S. (1991), "Helical microtubules of graphitic carbon", *Nature*, **354**(6348), 56-58.

Kolahchi, R., Hosseini, H. and Esmailpour, M. (2016a), "Differential cubature and quadrature-Bolotin methods for dynamic stability of embedded piezoelectric nanoplates based on visco-nonlocal-piezoelasticity theories", *Compos. Struct*., **157**, 174-186.

Kolahchi, R., Safari, M. and Esmailpour, M. (2016b), "Dynamic stability analysis of temperature-dependent functionally graded CNT-reinforced visco-plates resting on orthotropic elastomeric medium", *Compos. Struct*., **150**, 255-265.

Lei, J., He, Y., Guo, S., Li, Zh. and Liu, D. (2016), "Size-dependent vibration of nickel cantilever microbeams: Experiment and gradient elasticity", *AIP Adv*., **6**(10), 105202.

Li, S. and Wang, G. (2008), *Introduction to Micromechanics and Nanomechanics*, World Scientific Publication, Singapore.

Li, C. (2013), "Size-dependent thermal behaviors of axially traveling nanobeams based on a strain gradient theory", *Struct. Eng. Mech*., **48**(3), 415-434.

Li, L. and Hu, Y. (2016), "Wave propagation in fluid-conveying viscoelastic carbon nanotubes based on nonlocal strain gradient theory", *Comput. Mat. Sci*., **112**, 282-288.

Mirzaei, M. and Kiani, Y. (2016), "Free vibration of functionally graded carbon nanotube reinforced composite cylindrical panels", *Compos. Struct*., **142**, 45-56.

Mori, T. and Tanaka, K. (1973), "Average stress in matrix and average elastic energy of materials with misfitting inclusions", *Acta Metall. et Mater*., **21**(5), 571- 574.

Paliwal, D., Pandey, R.K. and Nath, T. (1996), "Free vibrations of circular cylindrical shell on Winkler and Pasternak foundations", *Int. J. Press. Vessel. Pip*., **69**(1), 79-89.

Qian, D., Dickey, E.C., Andrews, R. and Rantell, T. (2000), "Load transfer and deformation mechanisms in carbon nanotube-polystyrene composites", *Appl. Phy. Lett*., **76**(20), 2868-2870.

Qian, D., Wagner, G.J., Liu, W.K., Yu, M.F. and Ruoff, R.S. (2002), "Mechanics of carbon nanotubes", *Appl. Mech. Rev*., **55**(6), 495-533.

Razavi, H., Faramarzi Babadi, A. and Tadi Beni, Y. (2016), "Free vibration analysis of functionally graded piezoelectric cylindrical nanoshell based on consistent couple stress theory", *Compos. Struct*., **160**, 1299-1309.

Reddy, J.N. (2002), *Mechanics of Laminated Composite Plates and Shells: Theory and Analysis*, Second Edition, CRC Press.

Rogacheva, N. (1988), "Forced vibrations of a piezoceramic cylindrical shell with longitudinal polarization", *J. Appl. Math. Mech*., **52**(5), 641-646.

Saito, R., Dresselhaus, G. and Dresselhaus, M.S. (1998), *Physical Properties of Carbon Nanotubes*, Imperial College Press, London.

Shen, H.S. and Xiang, Y. (2012), "Nonlinear vibration of nanotube-reinforced composite cylindrical shells in thermal environments", *Comput. Methods Appl. Mech. Eng*., **213-216**, 196-205.

Shen, H.S. and Xiang, Y. (2014), "Nonlinear vibration of nanotube-reinforced composite cylindrical panels resting on elastic foundations in thermal environments", *Compos. Struct*., **111**, 291-300.

Shi, D.L. and Feng, X.Q. (2004), "The effect of nanotube waviness and agglomeration on the elastic property of carbon nanotube-reinforced composties", *J. Eng. Mat. Tech*., ASME, **126**, 250-270.

Song, Z.G., Zhang, L.W. and Liew, K.M. (2016), "Vibration analysis of CNT-reinforced functionally graded composite cylindrical shells in thermal environments", *Int. J. Mech. Sci*., **115**, 339-347.

Tadi Beni, Y., Mehralian, F. and Razavi, H. (2014), "Free vibration analysis of size-dependent shear deformable functionally graded cylindrical shell on the basis of the modified couple stress theory", *Compos. Struct*., **120**, 65-78.

Yas, M.H., Pourasghar, A., Kamarian, S. and Heshmati, M. (2013), "Three-dimensional free vibration analysis of functionally graded nanocomposite cylindrical panels reinforced by carbon nanotube", *Mat. Des*., **49**, 583-590.

Zeighampour, H. and Tadi Beni, Y. (2014), "Cylindrical thin-shell model based on modified strain gradient theory", *Int. J. Eng. Sci*., **78**, 27-47.

Zhang, L.W., Cui W.C. and Liew, K.M. (2015a), "Vibration analysis of functionally graded carbon nanotube reinforced composite thick plates with elastically restrained edges", *Int. J. Mech. Sci*., **103**, 9-21.

Zhang, B., He, Y., Liu, D., Shen, L. and Lei, J. (2015b), "Free vibration analysis of four-unknown shear deformable functionally graded cylindrical microshells based on the strain gradient elasticity theory", *Compos. Struct*., **119**, 578-597.

Zhang, B., He, Y., Liu, D., Shen, L. and Lei, J. (2015c), "An efficient size-dependent plate theory for bending, buckling and free vibration analyses of functionally graded microplates resting on elastic foundation", *Appl. Math. Model.*, **39**(13), 3814-3845.

CC